Published in final edited form as:
Antioxid Redox Signal. 2008 September ; 10(9): 1527–1548. doi:10.1089/ars.2008.2046.

Evolution of Catalases from Bacteria to Humans

Marcel Zamocky[1,2], **Paul G. Furtmüller**[1], and **Christian Obinger**[1]

[1] Department of Chemistry, Division of Biochemistry, BOKU-University of Natural Resources and Applied Life Sciences, Vienna, Austria.

[2] Institute of Molecular Biology, Slovak Academy of Sciences, Bratislava, Slovakia.

Abstract

Excessive hydrogen peroxide is harmful for almost all cell components, so its rapid and efficient removal is of essential importance for aerobically living organisms. Conversely, hydrogen peroxide acts as a second messenger in signal-transduction pathways. H_2O_2 is degraded by peroxidases and catalases, the latter being able both to reduce H_2O_2 to water and to oxidize it to molecular oxygen. Nature has evolved three protein families that are able to catalyze this dismutation at reasonable rates. Two of the protein families are heme enzymes: typical catalases and catalase–peroxidases. Typical catalases comprise the most abundant group found in Eubacteria, Archaeabacteria, Protista, Fungi, Plantae, and Animalia, whereas catalase–peroxidases are not found in plants and animals and exhibit both *catalatic* and peroxidatic activities. The third group is a minor bacterial protein family with a dimanganese active site called manganese catalases. Although catalyzing the same reaction ($2\ H_2O_2 \rightarrow 2\ H_2O + O_2$), the three groups differ significantly in their overall and active-site architecture and the mechanism of reaction. Here, we present an overview of the distribution, phylogeny, structure, and function of these enzymes. Additionally, we report about their physiologic role, response to oxidative stress, and about diseases related to catalase deficiency in humans.

Introduction

HYDROGEN PEROXIDE is one of the most frequently occurring reactive oxygen species in the biosphere. It emerges either in the environment or as a by-product of aerobic metabolism [*i.e.*, by oxygen activation (*e.g.*, superoxide formation and dismutation)] in respiratory and photosynthetic electron-transport chains and as product of enzymatic activity, mainly by oxidases. Both excessive hydrogen peroxide and its decomposition product hydroxyl radical, formed in a Fenton-type reaction, are harmful for almost all cell components. Thus, its rapid and efficient removal is of essential importance for all aerobically living prokaryotic (11) and eukaryotic cells (52). Conversely, hydrogen peroxide can act as a second messenger in signal-transduction pathways, mainly for immune cell activation, inflammation, cellular proliferation, and apoptosis (72, 76, 97). Evidence suggests that this signaling function of hydrogen peroxide was acquired rather late in evolution. In unicellular organisms, H_2O_2 mainly stimulates production of antioxidants and ROS-removing and repairing enzymes, whereas in multicellular organisms (both animals and plants), it is involved in activation of signaling pathways (83, 97).

Hydroperoxidases (catalases and peroxidases) are ubiquitous “housekeeping” oxidoreductases capable of the heterolytic cleavage of the peroxidic bond, predominantly in

Address reprint requests to: Marcel Zamocky Department of Chemistry, Division of Biochemistry BOKU-University of Natural Resources and Applied Life Sciences Muthgasse 18 A-1190 Vienna, Austria marcel.zamocky@boku.ac.at.

Europe PMC Funders Author Manuscripts

hydrogen peroxide (H-O-O-H), but also in some small organic peroxides (R-O-O-H; *e.g.*, ethyl hydroperoxide or acetyl hydroperoxide). Catalases have the additional striking ability to evolve molecular oxygen (O_2) by oxidation of hydrogen peroxide. Thus, enzymes with catalase activity degrade hydrogen peroxide by dismutation.

Several gene families evolved in the ancestral genomes capable of H_2O_2 dismutation. The most abundant are heme-containing enzymes that are spread among Bacteria, Archaea and Eukarya. They are divided in two main groups, typical or “monofunctional” catalases (E.C. 1.11.1.6, hydrogen peroxide, hydrogen peroxide oxidoreductase) and catalase–peroxidases. Both types of heme enzymes exhibit high catalase activities, but have significant differences, including absence of any sequence similarity and very different active-site, tertiary, and quaternary structures. Enzymatic classification of bifunctional catalase–peroxidases is not clear because, besides their *catalatic* activity (E.C. 1.11.1.6), they exhibit a peroxidase activity similar to that of conventional peroxidases (EC 1.11.1.7, hydrogen peroxide, donor oxidoreductase). Both protein families are present in prokaryotic and eukaryotic genomes. Nonheme manganese-containing catalases (Mn-catalases) constitute a third (minor) group of *catalatically* active enzymes. Mn-catalases (E.C. 1.11.1.6), initially referred to as pseudo-catalases, are present only in bacteria. The known sequences of all enzymes from these three protein families are collected and annotated in PeroxiBase (68; http://peroxidase.isb-sib.ch).

Investigation of heme enzymes with catalase activity has a very long documented history, going back to the 19th century (110). After the publication of the latter review, several new 3D structures of enzymes were solved, and new important mechanistic, functional, and physiologic aspects were published. It is, therefore, important to ask whether the data accumulated during the last decade led to a broadening of our knowledge concerning the diversity, enzymology, and physiologic role of these oxidoreductases in various organisms, most important, in humans. Here, we try to answer these most intriguing questions, including the role of catalases in symbiotic and host–pathogen interactions, as well as new aspects of catalase disorders in humans.

Catalase *Versus* Peroxidase Activity

Continuous and effective degradation of H_2O_2 is indispensable for aerobic life (110). This is essential both for removal of excessive H_2O_2 and for strict regulation of its concentration in signaling pathways (97). As mentioned earlier, nature has developed three protein families that can perform its dismutation at reasonable rates. The overall *catalatic* reaction includes the degradation of two molecules of hydrogen peroxide to water and molecular oxygen (reaction 1)

$$H_2O_2 \rightarrow 2\,H_2O + O_2 \quad \text{Reaction 1}$$

Reaction 1 is the main reaction catalyzed by typical catalases, catalase–peroxidases, and Mn-containing catalases. Additionally, several heme-containing proteins, including most peroxidases, metmyoglobin, and methemoglobin, have been observed to exhibit a low level of *catalatic* activity (64). From these enzymes, multifunctional chloroperoxidase from the ascomycete *Caldariomyces fumago* has the greatest reactivity as a catalase (95). Because of its very limited distribution in nature, this protein is not discussed here in more detail.

In catalases and catalase–peroxidases, two distinct stages can be distinguished in the *catalatic* reaction pathway. The first stage involves oxidation of the heme iron by using hydrogen peroxide as substrate to form compound I (reaction 2) (28). The oxygen–oxygen bond in peroxides (R-O-O-H) is cleaved heterolytically, with one oxygen leaving as water and the other remaining at heme iron (reaction 2). Generally, compound I is a redox

intermediate two oxidizing equivalents above the resting [*i.e.*, ferric, Fe(III)] state of the enzyme. In monofunctional catalases, compound I is an oxoiron(IV) porphyrin π-cation radical species [$^{\bullet+}$Por Fe(IV) = O], which is reduced back to the ferric enzyme by a second molecule of hydrogen peroxide, with the release of molecular oxygen and water (reaction 3). Thus, in a catalase cycle, H_2O_2 acts as oxidant (reaction 2) and reductant (reaction 3). Compound I can also undergo an intramolecular one-electron reduction with or without a proton, resulting in the formation of an alternative compound I (reaction 4) that is *catalatically* inactive. Here, the protein moiety (AA) donates the electron that quenches the porphyryl radical. Reaction 4 is responsible for the decrease of catalase activity with time, because the formed intermediate returns to the resting enzyme very slowly. A role of NADPH, which binds to some clades of monofunctional catalases, as two-electron donor for the transition of $^{\bullet+}$AA Por Fe(IV)-OH back to ferric catalase, has been discussed (see later).

$$\text{Por}\quad \text{Fe (III)} + H_2O_2 \rightarrow {}^{\bullet+}\text{Por}\quad \text{Fe (IV)} = O + H_2O \qquad \text{Reaction 2}$$

$${}^{\bullet+}\text{Por}\quad \text{Fe (IV)} = O + H_2O_2 \rightarrow \text{Por}\quad \text{Fe}\quad \text{(III)} + H_2O + O_2 \qquad \text{Reaction 3}$$

$$\text{AA}\ {}^{\bullet+}\text{Por Fe (IV)} = O + \quad H^+ \rightarrow {}^{\bullet+}\text{AA Por Fe (IV)} - \text{OH} \qquad \text{Reaction 4}$$

A lively debate exists about the question whether catalase–peroxidases also follow reactions 2 and 3. As in monofunctional catalases, organic peroxides (*e.g.*, acetyl hydroperoxide) can oxidize catalase–peroxidases to a compound I–like species according to reaction 2, which is rapidly transformed to a protein radical species (18, 42) with spectral UV-Vis signatures dissimilar to those described in monofunctional catalases (47). Thus, in the light of these data, a number of alternative reaction schemes for catalase–peroxidases have been proposed; these consider a rapid quenching of the porphyryl radical by an electron from the protein moiety. These alternative compound I species have been suggested to be $^{\bullet+}$MYW Fe(IV)-OH, or more generally, $^{\bullet+}$AA Fe(IV)-OH, with MYW being the catalase–peroxidase typical distal-side covalent adduct (see later), and AA being an alternative amino acid near the heme. In any case, also in catalase–peroxidases, the *catalatic* cycle has two distinct phases, with H_2O_2 acting as oxidant and reductant. In contrast to monofunctional catalases, this unique compound I species must be able to oxidize H_2O_2 (*i.e.*, it participates in the catalase cycle).

The mechanism of H_2O_2 degradation by nonheme Mn-catalases follows a completely different scheme. The overall reaction (reaction 1) also holds for these binuclear metallo-proteins, and again, H_2O_2 acts as oxidant and reductant, but the mechanism of the two individual reaction steps is completely different and is described later.

Catalases and catalase–peroxidases can also catalyze a peroxidatic reaction (reaction 5) in which electron donors (AH_2) are oxidized *via* one-electron transfers releasing radicals ($^{\bullet}$AH). Thus, a peroxidase cycle includes three reactions {*i.e.*, compound I formation [reaction 2], compound I reduction to compound II, an oxoiron(IV) species [PorFe(IV) = O; reaction 6], and compound II reduction back to the resting state (reaction 7)}. Generally, the peroxidatic reaction of monofunctional catalases is weak, but in bifunctional catalase–peroxidases, reaction 5 is important. Similar to the discussion of the catalase cycle, a dispute also exists about the electronic structure of redox intermediates of catalase–peroxidases in the peroxidase cycle (87).

$$H_2O_2 + 2\,AH_2 \rightarrow 2\,H_2O + 2\,{}^{\bullet}AH \quad \text{Reaction 5}$$

$$Por^{\bullet+}Fe(IV)=O + AH_2 \rightarrow Por\ Fe(IV)=O + {}^{\bullet}AH \quad \text{Reaction 6}$$

$$Por\ Fe(IV)=O + AH_2 \rightarrow Por\ Fe(III) + H_2O + {}^{\bullet}AH \quad \text{Reaction 7}$$

Peroxidatic reactions can also reduce compound I directly in a two-electron reaction back to the ferric enzyme (reaction 8). Especially mammalian and yeast catalases have been described to oxidize ethanol or other short-chain aliphatic alcohols to acetaldehyd or corresponding aldehydes (98, 110).

$$Por^{\bullet+}Fe(IV)=O + CH_3CH_2OH \rightarrow Por\ Fe(III) + CH_3CHO + H_2O \quad \text{Reaction 8}$$

In the following sections, we discuss the distribution and diversity of the three protein families (*i.e.*, typical catalases, catalase–peroxidases, and Mn-catalases) that are known to catalyse reaction 1 efficiently.

Distribution, Phylogeny, Structure, and Function of Typical ("Monofunctional") Catalases

Typical catalase is one of the most intensively studied heme enzymes in the last century (see 110 for details), with numerous publications on its occurrence and expression, structure, function, and modification. Analysis of prokaryotic and eukaryotic genomes reveals that genes coding for typical heme-containing catalases represent the largest group of hydrogen peroxide–degrading enzymes. Catalase has the Pfam accession number PF00199, and 943 DNA sequences (December 2007) currently contain this typical motif. Typical catalases are, strictly speaking, not monofunctional (as often designated in the literature) because besides H_2O_2, they can also perform two-electron oxidation reactions with other donors (see reaction 8). Moreover, recently these enzymes were described also to exhibit additional (*e.g.*, oxidase) activities (98). Nevertheless, the originally synonym "typical" catalase (56, 110) seems still to be the proper name for this protein family.

PeroxiBase presently contains 151 homologous protein sequences of typical catalases (in December 2007), and further related sequences will be annotated in the near future. The output of previous phylogenetic analysis revealed the existence of three main clades that were segregated rather early in the evolution of this gene family through at least two gene-duplication events (Figs. 1 and 2) (54).

Clade 1 contains eubacterial, algal, and plant catalases of small-subunit size (55–69 kDa) and heme *b* as the prosthetic group. Clade 2 contains large-subunit (75–84 kDa) catalases from eubacteria and fungi, with mainly heme *d* as the prosthetic group and an additional "flavodoxin-like" domain.

Clade 3 is the most abundant subfamily, and many bacteria possessing catalase gene paralogues of the first two clades also have a representative in the third clade. Clade 3 catalases also are found in archaebacteria, fungi, protists, plants, and animals. The

scientifically and medically important bovine liver and human erythrocyte catalases belong to clade 3. They are small-subunit (43–75 kDa) catalases containing heme *b* and NADPH as a second redox-active cofactor (see later).

As a particular example for this review, we analyzed the phylogenetic relationship of genes of *catalatically* active enzymes in cyanobacterial genomes. Cyanobacteria (blue–green algae) have evolved as the most primitive, oxygenic, plant-type photosynthetic organisms. They were the first that produced molecular oxygen as a by-product of photosynthetic activity. Today they live in habitats with potentially damaging photooxidative conditions due to high irradiation and oxygen concentrations. Because in evolutionary history, they were responsible for accumulation of molecular oxygen in a so-far reducing atmosphere, they must have been among the first organisms that developed strategies to cope with reactive oxygen species (ROS) produced by incomplete reduction of molecular oxygen *via* electron-transport processes. Interestingly, genes for typical catalases are very unusual in cyanobacteria (see http://bacteria.kazusa.or.jp/cyanobase/ for details and updates). At the moment, the only complete and nonfused gene in which all essential parts are conserved is found in *Nostoc punctiforme* [NopuKat01, entry 5534 in PeroxiBase; (68) and references therein] and, as is obvious from Fig. 2, it belongs to clade 3 of small-subunit catalases with a high bootstrap support. Another cyanobacterial protein of this family (NOspKatOx01 = entry 5629 in PeroxiBase) is part of a fusion protein between a typical catalase-related domain and a putative lipoxygenase domain, with significant similarity to the well-investigated fusion protein of allene oxide synthase from *Plexaura homomalla* and related corals (66). In NopuKat01, the phylogenetic analysis suggests a lateral gene transfer (LGT) from an ancestral proteobacterium to *Nostoc punctiforme* (Fig. 2). In the fusion protein, the corresponding cyanobacterial gene has a common ancestry with corresponding genes of marine metazoans. As is demonstrated later, the main *catalatically* active enzymes in cyanobacteria are catalase–peroxidases or Mn-catalases or both.

Until now, fourteen 3D structures of typical heme catalases in native and oxidized form have been solved, including bacterial (1), fungal (61) and mammalian (74) proteins. It should be mentioned that a heme catalase was among the first proteins crystallized by Sumner and Dounce in 1937 (110). Table 1 provides an overview of all available 3D structures of typical catalases. All known typical catalases are homotetrameric enzymes with 222 point-group symmetry (14, 37). Each subunit of clade 1 and 3 proteins contains a protoporphyrin IX containing Fe(III) (*i.e.*, heme *b*). Only in clade 2 proteins with large subunits is heme *b* autocatalytically transformed to heme *d* through dihydroxylation at the C5-C6 double bond of pyrrole ring III, followed by *cis*-γ-spiro-lactone formation in position C6 (24). Figure 3 depicts two representative structures of both a small-subunit heme *b* and a large-subunit heme *d* catalase. Four invariant residues are found in all typical catalases sequenced so far: the distal residues histidine, asparagine (rare exception: PnoKat01 from the ascomycete *Phaeosphaeria nodorum*), and serine and the proximal heme iron ligand tyrosine. Although the architecture of the active center is nearly perfectly conserved throughout the evolution (Fig. 1A and C), a significant difference exists in the overall fold between small- and large-subunit catalases (Fig. 1B and D). The main differences are located on the N-terminal arm and in the presence of an extra C-terminal flavodoxin-like domain in large catalases.

In all *catalatically* active enzymes, the architecture of substrate channel(s) leading to the deeply buried active center has been shown to play a crucial role, especially in reaction 3 (*i.e.*, H_2O_2 oxidation). In *Saccharomyces cerevisiae* catalase A (a model for all clade 3 catalases), classic molecular interaction potentials, molecular dynamics, and activated molecular dynamics calculations (51) clearly demonstrated that water can be a competitive inhibitor of catalase *via* blocking the access of hydrogen peroxide to the active site. The main channel, located perpendicular to the plain of the heme, was shown to be the preferred

route for H_2O_2 access to the active site in a majority of known catalase structures (*e.g.*, 16). The overall affinity of the main channel for binding of molecules of H_2O_2 is only slightly higher than that for H_2O. Changes to the largely hydrophobic residues in the lower part of the channel just above the heme or generally enlarging the channel by exchanging bulky residues with smaller amino acids causes a decrease in the catalase and an increase in the peroxidase activity of typical catalases (60). This underlines the importance of evolutionary-optimized shape and size of substrate channels in *catalatically* active enzymes. Similar considerations also apply for catalase–peroxidases and manganese catalases (see later). The structures of typical catalases reveal two additional minor channels leading from the surface to the active site. Regarding the rapid turnover rate of catalases, they could function as separate inlet and outlet channels, allowing rapidly evolving oxygen to be removed without interfering with incoming H_2O_2 (17).

The reaction mechanism of typical catalases was investigated in detail by several groups (23, 28, 36, 37, 40). It is generally accepted that H_2O_2 dismutation occurs at the distal heme cavity, according to reactions 2 and 3. Hydroperoxide initially associates in the active site with heme Fe(III) and forms a hydrogen bond with the conserved distal histidine (Figs. 1 and 3), which has its imidazole residue coplanar with the heme. This stretches the O-H bond, allowing the second oxygen of the peroxide also to form a hydrogen bond with the imidazole. The proton of the oxygen bound to the iron is then transferred, *via* the imidazole, to the second oxygen, giving rise to water and compound I (64). The role of the conserved distal asparagine (Fig. 3) is to stabilize and polarize the peroxide. Compound I in typical catalases is an oxoiron(IV) porpyrin π-cation radical species (6).

In compound I reduction (*i.e.*, H_2O_2 oxidation to O_2), the second H_2O_2 binds to compound I, forming hydrogen bonds with the oxoiron(IV) oxygen, the distal histidine, and asparagine (28). This allows the transfer of one hydrogen to the oxoiron(IV) and a second to the imidazole, resulting in formation of molecular oxygen. The hydrogen and second reducing equivalent on the imidazole ring could then be transferred to the Fe(IV)=O to produce water and native ferric catalase (63).

In all typical catalases, the proximal heme iron ligand is a tyrosinate (Figs. 1 and 3) that modulates heme iron reactivity and stabilizes higher oxidation states (99). Its participation in redox reactions is also reflected by its unusual modifications in some catalases. In *Escherichia coli* HPII, the N^{δ} of the imidazole ring of a proximal histidine has been shown to be covalently linked with the C^{β} of the essential tyrosine (8). Its role could be to enhance resistance to peroxide, thereby stabilizing the enzyme at high turnover rates at high peroxide concentrations and to avoid formation of *catalatically* inactive compound II. Similarly, in *Neurospora crassa* CAT-1, a Tyr-Cys covalent bond was detected (24). Many other unusual modifications in typical catalases have been described (64).

Among catalases, reaction rates and substrate affinities can differ significantly (90). Generally, *catalatically* active enzymes do not follow Michaelis–Menten kinetics except at very low substrate concentrations, and different enzymes are affected differently at higher substrate concentrations. Most small-subunit enzymes are inactivated by H_2O_2 concentrations >300–500 m*M* and never reach the Michaelis–Menten v_{max} predicted by extrapolation from rates at low substrate concentrations. Conversely, large-subunit enzymes are inhibited only at very high hydrogen peroxide concentrations (>500 m*M*; 90). Thus, presentation of K_m and v_{max} values in the literature is problematic. Nevertheless, apparent values are reported to vary from 54,000 to 833,000 per second for k_{cat} and 38 to 600 m*M* for K_m (17). The activities of typical catalases are essentially pH independent from pH 5 to pH 10.

Some typical catalases are among the rare group of enzymes possessing two distinct prosthetic groups within one enzyme subunit: heme and NADPH, the latter being bound only to clade 3 catalases. The order of affinities is NADPH > NADH > $NADP^+$ > NAD^+, with one nucleotide bound per monomer. The nucleotide is not a compulsory cofactor of the catalase activity, and many small-subunit catalases lose NADPH during purification. Principally the structural adjustments required for nucleotide binding are minor. NADPH binds in a compact structure at a site ~20 Å from the heme iron in a highly conserved environment (Fig. 4).

The role of NADPH is still under discussion. As was outlined earlier, typical catalases form an alternative compound I by intramolecular electron transfer (reaction 4), which is inactive in H_2O_2 oxidation. Inactivation could occur at very low H_2O_2 concentrations, where compound I exists for a longer time before another H_2O_2 converts it back to the resting state. It has been proposed that NADPH serves as an electron source by directly converting this intermediate back to the resting state, thereby circumventing inactivation (40). This fits with the observation that in large-subunit catalases, which lack NADPH binding, quenching of the porphyryl radical by intramolecular electron transport has never been found. It has been speculated that the compact NADPH structure in catalases may allow more-effective electron transfer donation from the nicotinamide while still allowing the adenine ring to serve as an anchor for the nucleotide on the enzyme surface (Fig. 4) (64).

Two recent findings should be mentioned. At low peroxide concentrations, bovine catalase has been reported to have the ability to consume hydrogen peroxide without generating O_2 (22). In the presence of NADPH, reaction 4 was not observed. But in the absence of NADPH, both reaction 4 and H_2O_2 consumption occurred, suggesting that the catalase has reducing groups within its own protein moiety for recovering the native enzyme (22). Studies with ^{14}C-labeled NADPH also demonstrated that bound NADPH is not displaced from catalase on oxidation. It was thus proposed that bovine liver catalase must have a reductase and transhydrogenase activity for regeneration of bound NADPH (30).

Recently, it was suggested that both purified mammalian catalase and cells expressing this enzyme could use released molecular oxygen for a unique oxidase activity (98). The authors found that the thermal stability of oxidase activity corresponded to that of catalase activity and that the oxidation reaction was distinct from a classic peroxidase reaction (98). Indole derivatives have been suggested as oxidase substrates, and a potential binding site has been addressed in the crystal structure of human catalase (74, 98). It was proven that eukaryotic typical catalases are involved not only in the degradation of hydrogen peroxide but also in inhibition of cellular redox signaling (80, 97).

Distribution, Phylogeny, Structure and Function of Catalase–Peroxidases

Bifunctional catalase–peroxidase (KatG) has raised considerable interest, because it represents the only peroxidase with a reasonably high *catalatic* activity around neutral pH (reaction 1), besides a usual peroxidase activity (reaction 6). Its overall fold and active-site architecture is typical peroxidase-like, which is underlined by their striking sequence homologies to other members of class I of one heme peroxidase superfamily (102). Together with these peroxidases (*i.e.*, ascorbates peroxidases and cytochrome *c* peroxidase), KatGs have the Pfam accession number PF00141. The InterPro accession number IPR000763 is more specific only for catalase–peroxidase.

PeroxiBase currently (December 2007) contains 329 sequences of *katG* genes, and their evolution was analyzed recently (69). The most important output of this investigation is that *katG* genes are distributed in ~40% of bacterial genomes and sometimes even closely-related species differ in possessing *katG* genes of different origin or even do not possess any *katG*

gene. Two different evolutionary lines of *katG* genes also exist in eukaryotes: one in algae, and one in fungi, and both are expected to originate from lateral gene transfer of corresponding bacterial genomes living in close relation with the eukaryotes (69, 109). Phylogenetic analysis reveals that the closest neighbor of all fungal *katG* genes is the *katG* gene of *Flavobacterium johnsonii* (Fig. 6). In fungal KatGs, two clades are found, one encoding cytosolic, and the other, secreted enzymes. The occurrence of extracellular fungal KatGs is underlined by the prediction of signal sequences.

The four available crystal structures (Table 1) of the KatGs *Haloarcula marismortui* (1ITK) (106); *Burkholderia pseudomallei* (1MWV) (12), *Mycobacterium tuberculosis* (1SJ2) (7), and *Synechococcus* PCC 7942 (1UB2) (100) revealed that the homodimeric heme *b* enzymes have proximal and distal conserved amino acids at almost identical positions as in other class I peroxidases (Fig. 7). In particular, both the triads His/Trp/Asp (His279, Trp330, and Asp389; *Burkholderia* numbering) and His/Arg/Trp (His112, Arg108, Trp111) are conserved (Fig. 5). Moreover, the proximal His is hydrogen bonded to the carboxylate side chain of the nearby Asp residue, which, in turn, is hydrogen bonded to the nitrogen atom of the indole group of the nearby Trp residue (Fig. 7). However, the x-ray structures also revealed features unique to KatG. In the vicinity of the active site, novel covalent bonds are formed among the side chains of three distal residues, including the conserved Trp111 (Figs. 5 and 7). In particular, both x-ray crystallization data (Table 1) and mass spectrometric analysis (25, 45) confirmed the existence of a covalent adduct between Trp111, Tyr238, and Met264 (Fig. 7). Exchange of either Trp111 or Tyr238 prevents cross-linking, whereas exchange of Met264 still allowed the autocatalytic covalent bond formation between Trp111 and Tyr238 (31, 45).

In addition to an extra C-terminal copy resulting from gene duplication (102), which lacks the prosthetic group but supports the architecture of the active site (3), other KatG-typical features are three large loops; two of them show highly conserved sequence patterns (111) and constrict the access channel of H_2O_2 to the prosthetic heme *b* group at the distal side. The channel is characterized by a pronounced funnel shape and a continuum of water molecules. At the narrowest part of the channel, which is similar but longer and more restricted than that in other monofunctional peroxidases, two highly conserved residues, Asp141 (Fig. 7) and Ser324 control the access to distal heme side. Together with a conserved glutamate residue at the entrance, both acidic residues seem to be critical for stabilizing the solute matrix and orienting the water dipoles in the channel. Exchange of both residues affects the catalase but not the peroxidase activity. It is interesting to note that in typical catalases, similar acidic residues participate in stabilization and orientation of the solute matrix in the main access channel for H_2O_2.

This extensive distal-site hydrogen-bonding network causes KatGs to differ from typical peroxidases. Typically, the *catalatic* but not the peroxidatic activity is very sensitive to mutations that disrupt this network (39, 44). Moreover, the integrity of this network is crucial for the formation of distinct protein radicals that are formed on incubation of KatG with peroxides (42, 43). Mutational analysis clearly underlined the importance of the KatG-typical covalent adduct Trp-Tyr-Met. Its disruption significantly decreased the catalase but not the peroxidase activity. For instance, on exchange of Tyr238 by Phe, the resulting KatG variant completely lost its capacity to oxidize H_2O_2 and was transformed to a typical peroxidase (43). Similarly, all other mutations so far performed in the heme cavity or substrate channel of a KatG affected the oxidation and not the reduction reaction of hydrogen peroxide (87), which is the initial reaction in all heme hydroperoxidases.

Hydrogen peroxide reduction (*i.e.*, compound I formation) follows reaction 2, which—in contrast to typical catalases—is immediately followed by reaction 4, forming the

catalatically active intermediate $^{\bullet+}$AA Por Fe(IV)-OH, with AA being the so-far unlocalized amino acid radical. Here, it is important to note that the exact electronic structure of this compound I species, which actually oxidizes H_2O_2, is still speculative (47). One role of the Trp-Tyr-Met adduct could be the (at least transient) radical site ($^{\bullet+}$MYW Fe(IV)-OH) that quenches the porphyryl radical. Similar to typical peroxidases, compound I formation (*i.e.*, the heterolytic cleavage of H_2O_2) is clearly assisted by the conserved distal residues His112 and Arg108 (87), but the exact role of distal amino acids in H_2O_2 oxidation is unknown.

Both K_m and k_{cat} values of KatGs are significant lower compared with those of typical catalases. Apparent values range from 3,500 to 6,000 per second and 3.7 to 8 m*M* (87). In contrast to typical catalases and Mn-catalases, the catalase activity of KatG has a sharp maximum activity around pH 6.5.

KatG is a bifunctional enzyme. It oxidizes typical artificial peroxidase substrates like *o*-dianisidine, guaiacol, or ABTS. The pH profile of the peroxidase activity of KatG has its maximum around pH 5.5, independent of the nature of most donors. Compound I (formed with peroxoacetic acid) reduction by monosubstituted phenols and anilines has been shown to depend on the substitution effect on the benzene ring and follows the Hammet equation (77), similar to typical peroxidases. Additionally, KatGs have been reported also to have halogenation (46) and NADH oxidase (86) activity.

The naturally occurring peroxidase substrate is unknown. In physiologic conditions, it is well known that KatG from *Mycobacterium tuberculosis* can activate the antituberculosis drug isoniazid (112), but otherwise the physiologic function of these enzymes remains unknown. Because of the restricted access, only small peroxidase substrates can enter the main entrance channel. A second access route, found in monofunctional peroxidases, approximately in the plane of the heme, is blocked by the KatG-typical loops. However, another potential route that provides access to the core of the protein, between the two domains of the subunit, has been described (12). It has been speculated that this could be the binding site for substrates with extended, possibly even polymeric character. In any case, neither from prokaryotic nor from eukaryotic KatGs is the naturally occurring one-electron donor(s) known nor is the function of a high peroxidase activity in a *catalatic* enzyme. A reasonable role at low peroxide concentration could be the reduction of alternative and *catalatically* inactive compounds I and II species to ferric KatG (similar to NADPH in clade 3 catalases). The potential role of catalase–peroxidases in H_2O_2 signaling remains elusive and must be investigated on both transcriptional and translational levels. This is an actual topic mainly for eukaryotic catalase–peroxidases, as possible signaling pathways can exist mainly during the interaction between host and pathogen.

Distribution, Phylogeny, Structure, and Function of Manganese Catalases

Manganese catalases (Mn- or nonheme or dimanganase catalases) represent only a minor gene family. Currently (December 2007), in PeroxiBase, 30 representatives are known, and all of them originate in bacterial genomes. This protein family has the signatures PF05067 and IPR007760 belonging to the ferritin-like superfamily comprising also desaturases, ferritins, and phenol hydroxylases. Phylogenetic analysis reveals the presence of five distinct and well-segregated clades (with a high bootstrap support; Fig. 8). Lateral gene transfer occurred during the evolution of this protein family between various bacterial taxa. Clade 1 includes archaebacterial proteins and at least one Firmicutes representative. Clade 2 is distributed among the taxa of Actinomycetes and Firmicutes. Clades 1 and 2 share a common ancestor (Fig. 8). Clade 3 is spread among Firmicutes and Proteobacteria, whereas clade 4 was separated rather early from the common ancestor of all the mentioned clades. Its representatives occur mainly in genomes of the genus *Bacteroides* and in several

cyanobacteria. In clade 5, proteobacterial sequences are found. It seems to be most distantly related to all other clades and diverted early in the history of this gene family.

Multiple-sequence alignment reveals a rather high identity, mainly in the active-site residues. This is underlined by the so-far known three-dimensional structures of two distinct representatives [Table 1; *i.e.*, Mn-catalase from *Thermus thermophilus* (2) and *Lactobacillus plantarum* (4)]. The enzymes contain six identical subunits (~30 kDa), each with a bridged binuclear Mn-center located within a conserved closely packed four-helix bundle domain (Fig. 9). The ligands for the dimanganese center are almost invariantly conserved among all known sequences (Fig. 10). A bridging glutamate (Glu66 in LplMnCat01) anchors the two ions in the binuclear cluster. Each Mn ion is further coordinated by one histidine (His69 to Mn1 and His181 to Mn2) and one glutamate (Glu35 to Mn1 and Glu148 to Mn2) bound to opposite faces of the cluster (Fig. 9) (104). These essential ligands are highly conserved, forming typical signatures of the MnCat sequence (Fig. 10), whereas the environments of these ligands differ slightly. The manganese core is completed by two solvent-derived oxygen atom bridges. The presented sequence alignment (Fig. 10) suggests that in the *Bacterioides* enzyme BcapMnCat, an aspartate could act as a ligand instead of a histidine (Fig. 10).

Access to the binuclear center is *via* a central channel that extends the full width of the hexamer, with branches into each subunit. Each dimanganese center is embedded in a network of hydrogen bonds that radiate from the metal center toward the outer-sphere environment. The length (≈15 Å) and narrowness of these channels are strongly reminiscent of typical catalases and catalase–peroxidases. Again, a restricted access to the only substrate hydrogen peroxide is very important for the *catalatic* reaction. Because heterologous expression in *E. coli* was not successful, a homologous plasmid expression system in *Lactobacillus plantarum* was established (104). Mutational analyses of an essential outer-sphere tyrosine (Tyr 42), which is conserved in all available sequences clearly demonstrated the importance of an intact hydrogen-bonding network also in Mn-catalases (104). In the variant Tyr42Phe, a solvent bridge was broken, and an “open” form of the dimanganese cluster was generated, thereby considerably influencing the catalytic turnover, pH optimum, and interaction with H_2O_2.

The catalatic reaction in manganese catalases differs significantly from that in both typical catalases and catalase–peroxidases. The dimanganese cluster is equally stable in either Mn^{2+}-Mn^{2+} or Mn^{3+}-Mn^{3+} oxidation states. On isolation, the protein is frequently in a mixture of both oxidation states. Fully reduction to Mn^{2+}-Mn^{2+} is mediated by hydroxylamine, whereas reoxidation to a homogeneous Mn^{3+}-Mn^{3+} state can be achieved by molecular oxygen at pH >7.0 (103). The *catalatic* reaction can be written as a two-stage process. During catalytic turnover, the active site has to accommodate both the reduced and the oxidized state of the dimanganese core. The Mn^{2+}-Mn^{2+} cluster is expected to polarize the O-O bond, favoring a heterolytic cleavage of the peroxidic bond and release of water (reaction 9) (104). Hydrogen peroxide oxidation and dioxygen release occurs by a simple electron transfer (reaction 10). Principally, no temporal order exists in the reduction and oxidation stages.

$$H_2O_2 + Mn^{2+} - Mn^{2+}\ (2H^+) \rightarrow Mn^{3+} - \begin{matrix} Mn^{3+} \\ +2\,H_2O \end{matrix} \quad \text{Reaction 9}$$

$$H_2O_2 + Mn^{3+} - Mn^{3+} \rightarrow Mn^{2+} - Mn^{2+}\ (2H^+) + O_2 \quad \text{Reaction 10}$$

It is assumed that the change in the oxidation status is responsible for protonation or deprotonation of both bridging oxygens. Protonation is proposed for the reduced Mn^{2+}-Mn^{2+} state (see reaction 9), which is in line with an observed drastic reduction of the magnetic exchange coupling between the two Mn^{2+} ions (94). In contrast to heme-containing catalases, no reactive intermediate is formed, and both product waters are formed in one reaction (reaction 9). No evidence exists for involvement of free radicals in manganese catalase turnover, and nothing is known about peroxidatic reactions with one- and two-electron donors. Recently, manganese catalases have been subjected to molecular dynamics calculations, allowing the detailed reconstruction of the reaction mechanism and comparison with a *de novo* biomimetic dimanganese protein analogue (88).

The H_2O_2 dismutation rates are lower compared with typical catalases and catalase–peroxidases, which could explain why Mn-catalases may not have become as widespread in nature. The activity varies only slightly over the pH range from 5 to 10, very similar to typical catalases. The apparent K_m values are reported to be ~220 m*M* (104), suggesting a low catalytic efficiency at low H_2O_2 concentrations. Their exact physiologic role(s) and expression pattern are more or less unknown. This clearly implies that the only hypothetical role of manganese catalases in H_2O_2 signaling must be investigated on both transcriptional and translational levels.

Physiologic Role and Expression of Typical Catalases and Catalase–Peroxidases as a Response to Oxidative Stress

Of several definitions of oxidative stress, the most appropriate regarding the role of antioxidant enzymes is that oxidative stress is “a disruption of redox signaling and control” (50). Both typical catalases and catalase–peroxidases are known to belong to the constitutive enzymatic armory against oxidative stress or are expressed as a response to it or both. The role of both these groups in H_2O_2 signaling can be proposed but, mainly in the case of KatGs, it still must be comprehensively investigated. The whole aerobically living world from bacteria to higher eukaryotes has to maintain H_2O_2 concentrations at nonharmful levels. Many experimental data on this topic have been published. A few typical examples are presented here.

Contrary to earlier suggestions, even some obligate anaerobes are known to contain typical catalase(s). Certain butyric fermentation bacteria of the genus *Clostridium* express catalase, mainly in their spores. The addition of hemin significantly enhances the expression of catalases in *C. acetobutyricum* (9). Many species of the strict anaerobic genus *Bacteroides* are catalase positive. The catalase-free mutant of *B. fragilis* exhibits increased sensitivity to hydrogen peroxide, explaining the resistance of wild-type *B. fragilis* (among the most aerotolerant strict anaerobes) to oxygen (79). Catalase activity was also found in several *Desulfovibrio* strains. The typical catalase from *D. gigas* is constitutively expressed, but probably it is not fully saturated with the prosthetic heme group (26). The strict anaerobe *Methanobrevibacter arboriphilus* also exhibits catalase activity with a maximum in the stationary phase of growth. This catalase activity is significantly enhanced on addition of hemin in the growth medium, and the purified protein has many properties of typical catalases (84). Another example is the expression of KatA from *Helicobacter hepaticus*. This proteobacterial typical heme catalase was shown to play an important role in oxidative-stress resistance of this dangerous pathogen of mammalian liver. A catalase mutant deficient in corresponding chromosomal locus was not able to grow at elevated oxygen levels and exhibited a marked hypersensitivity in conditions of oxidative stress (41). Additionally, the catalase mutant exhibited severe DNA fragmentation after treatment with sublethal concentrations of hydrogen peroxide.

In most (eu)bacteria that possess catalase gene paralogues in their genomes, only one enzyme is specifically induced by oxidative stress. *Bacillus subtilis* contains two genes encoding typical catalases, with KatA being oxidative stress induced and KatE (and its homologues in other bacteria) being a general (σ-B dependent) stress protein (27). Regarding the physiology of catalase expression and its control in bacteria, *Escherichia coli* is well studied. *E. coli* contains two *catalatically* active enzymes, a catalase–peroxidase (HPI) and a typical catalase (HPII). KatG (HPI) is mainly expressed on induction of oxidative stress, whereas expression of the monofunctional catalase is increased as cells grow into stationary phase. HPI is controlled as part of the OxyR regulon, which senses active oxygen species. HPII is controlled as part of the σ^S regulon in stationary phase, and its role seems to be protection during periods of slow or no growth (62).

Generally, symbiotic and pathogenic organisms contain an increased number of catalase gene paralogues. In the completely sequenced genome of the soil bacterium *Sinorhizobium meliloti*, three genes encoding *catalatically* active heme proteins can be found (48). Two monofunctional catalases, KatA (small subunits) and KatC (large subunits), and a catalase–peroxidase (KatG) are expressed in *S. meliloti.* This soil bacterium is able to develop a symbiosis with some *Medicago* species, and such plant–bacterium interaction leads to the formation of root nodules (57). During this process, bacteria differentiate. The expression of the three heme enzymes is differentially regulated both during the development of the nodule and in the different phases of growth of the free-living cells. In the latter, only KatA is expressed by exposure to H_2O_2. Induction of KatC depends on heat stress, salt stress, and ethanol, whereas induction of KatG is not induced by any of the tested treatments (48, 85). Mutational studies clearly demonstrated the importance of this armory of H_2O_2-detoxifying enzymes in the symbiotic process with the plant (48).

As outlined earlier, genomes of oxygenic phototrophic cyanobacteria show the presence of KatGs or Mn-catalases or both, whereas typical catalases are uncommon. In phototrophic organisms, severe oxidative stress is induced by high-light illumination. Surprisingly, catalase–peroxidase of *Synechococcus* sp. strain PCC 7942 (and in similar way, KatG of *Synechocystis* strain PCC 6803) is dispensable for survival, as indicated by mutant growth experiments (70). The authors of this study suggest that a thioredoxin-dependent peroxidase is crucial in light-induced oxidative stress. In contrast, cyanobacterial KatG is essential for survival and the elimination of relatively high concentrations of externally added H_2O_2 (70), a fact that underlines the predominant *catalatic* function of KatG *in vivo*. The genomes of both mentioned cyanobacterial species do not contain genes encoding Mn-catalases.

In the fungus *Neurospora crassa*, catalase-1 (a typical catalase) plays–together with a diphosphate kinase (NDK-1)–an essential role for the survival of conidia under oxidative and light-induced stress, including singlet oxygen. ROS are reported to play an important role in light-mediated signal transduction (101), and *N. crassa* catalase-1 seems to be involved in this cascade.

In the yeast *S. cerevisiae*, two typical catalases, an organelle-located KatA and a cytosolic KatT, have been identified. Both are highly expressed under conditions that induce peroxisome formation. Recently, it was demonstrated that KatA is targeted to both peroxisomes and the mitochondrial matrix (71). This finding is surprising, because catalase A is well known to contain two distinct peroxisomal targeting signals (55), but it lacks a classic N-terminal mitochondrial import sequence. Nevertheless, mitochondrial and peroxisomal co-import was monitored in *Saccharomyces cerevisiae*, both qualitatively by fluorescence microscopy and functional complementation, and quantitatively by Western blot analysis of subcellular fractions and by activity assays. Increased import of catalase A in mitochondria was observed mainly when the culture was subjected to intensive

respiration that favors oxygen activation and finally H_2O_2 accumulation. Generally, mitochondrial targeting was favored in cultures grown on nonfermentable carbon sources (71).

Catalases in fungi, which are pathogenic for humans, have been studied intensively in recent years. During the unspecific immune response, the so-called respiratory burst is induced, thereby releasing superoxide from special activated leukocytes. As a consequence, high concentrations of hydrogen peroxide are formed that must be overcome by the phytopathogenic fungi. *Aspergillus fumigatus* can express three *catalatically* active enzymes (67). One catalase is a clade-2 large-subunit, monofunctional, and heat-stable catalase and is located in conidia. In contrast to the two other mycelium-located enzymes, it is not a virulence factor. Both mycelial proteins (a KatG and a typical catalase) have been shown to be involved in the protection of this ascomycete against the oxidative burst in an experimental rat model (67). Recently, an inducible KatG from the dangerous human pathogen *Penicillium marneffei* was isolated and partially characterized (73). In two important phytopathogenic fungi, *Gibberella zeae* and *Magnaporthe grisea*, six and five distinct genes coding for typical catalases and catalase–peroxidases exist (http://peroxidase.isb-sib.ch). Their physiologic role and possible inducible expression is currently under investigation (109). But *catalatically* active enzymes also protect the host from pathogenic attack. Recent experiments in culture plants reveal that catalase activity of the host is directly associated in interactions leading to the resistance of maize to the infection caused by *Aspergillus flavus* (58).

The presence of typical catalases in peroxisomes is well known. Older studies in mammalian cultures revealed the presence of catalase activity in rat-heart mitochondria, where it was identified as a key antioxidant defense system of myocardium (75). Recent findings support the occurrence of typical catalases in mitochondria of insect (5) as well as mammalian cells (81). The constitutive presence of an endogenous heme catalase inside mitochondria was demonstrated by subcellular fractionation, proteinase K sensitivity, and immunogold electron microscopy on both isolated rat liver mitochondria and on the whole-rat liver tissue (81). Mitochondrial catalase has a preventive role mainly against membrane lipid alterations, inactivation of respiratory chain components, mutations and strand breaks in mitochondrial DNA, and opening of permeability transition pores by hydrogen peroxide. Recent physiological data from overexpression of catalase in transgenic mice reveal a protective function of heme catalase in cardiomyocytes against aging-induced contractile defects and protein damage (105).

Diseases Caused by Catalase Deficiency and Overexpression

Catalase deficiency can originate from too-low or too-high expression levels and improper folding, assembly, and function of the human enzyme and can be related to rapid changes in the physiologic H_2O_2 concentration, altered peroxide signaling pathways, and inefficient targeting to peroxisomes (92) and mitochondria (71). Even further cellular organelles like endoplasmic reticulum, nucleus, and plasma membrane have been reported to be affected by catalase deficiency (107).

Human erythrocytes are usually exposed to substantial amounts of oxygen. As a consequence of metabolic activity of various oxidases (mainly involved in the β-oxidation of fatty acid chains), hydrogen peroxide is generated in a rather high concentration. Hemoglobin is protected by catalase colocalized in the erythrocytes (29). In erythrocytes that lack catalase, ferrous hemoglobin is oxidized with hydrogen peroxide to methemoglobin [*i.e.*, Por Fe(III)] and, finally, to an oxoiron(IV) species, Por Fe(IV)=O, with protein-based

radical(s). As a consequence, hemolysis of erythrocytes, polymerization of haemoglobin, and aggregation of malfunctioned erythrocytes is observed (59).

Catalase was shown to prevent the redox-sensitive nuclear transcription factor NF-êB from activating a cascade leading to lung inflammation through rapid regulation of physiologic ROS levels (76). It was also observed that cancer cells generate abnormally high H_2O_2 levels because of substantially low catalase activities compared with normal cells (89). After the detection of the formation of a complex between Grb2–a growth factor–binding protein– and the motif ^{447}Tyr-Val-Asn-Val in human catalase, it was proposed that catalase participates in integrin signaling (107). The binding of Grb2 occurs specifically on phosphorylation in tumor cells when stimulated with serum or ligands. On binding to catalase, the specific catalase activity was modified (108). These results propose indirect involvement of complexed catalase in the regulation of cell proliferation.

The human genetic disease related to loss of functional catalase is generally known as acatalasemia, or Takahara disease (65). Acatalasemia, spread in human lineages as inherited deficiency, has been detected in 113 cases in 59 families from 11 countries worldwide (33). In a strict sense, we have to distinguish between acatalasemia and hypocatalasemia. Whereas hypocatalasemia is heterozygous and leads to a ~50% reduction of catalase activity, acatalasemia is homozygous, and the overall catalase activity is decreased to <10% of normal level. Such a low value is critical for many physiologic processes. Patients from Japan, Switzerland, and Hungary were investigated intensively by using clinical, biochemical, and molecular genetic methods. The frequency of acatalasemia was determined to be 0.04:1,000 in Switzerland, 0.05:1,000 in Hungary, and 0.8:1,000 in Japan. The frequency of hypocatalasemia is 2.3:1,000 in Hungary and 2–4:1,000 in Japan (32). In other countries, the identification of acatalasemia types was only sporadic.

Obvious differences in detected mutations exist among Japanese, Swiss, and Hungarian types of acatalasemia. In the Swiss type, a truncated catalase protein is found (20). Comprehensive analysis of all detected mutations in the catalase gene was performed (33). Not all of them lead to a significant modification of the catalase protein structure; some are regulatory mutations resulting in a less-stable protein. The recently found single-base substitution in exon 9 leading to the exchange Arg354Cys in Hungarian type D acatalasemia is very likely to cause a drastic decrease in blood catalase activity (35). Inspection of Fig. 1B shows that this type of acatalasemia leads to an exchange of a highly conserved arginine involved in a characteristic motif around the proximal tyrosine. Arginine 354 favors the ionization of the hydroxyl group of proximal Tyr358, and its exchange by cysteine disturbs the proper folding of the active site, thereby leading to the dramatically decreased activity in type D acatalasemic patients (35).

The most frequently occurring clinical features of acatalasemia include oral gangrene; ulceration; altered lipid, saccharide, and homocysteine metabolism (homocysteinemia); and an increased risk of diabetes mellitus. All these features reveal a high incidence in childhood, and some of them lead to a shortened lifespan, also connected with various forms of cancer in adult persons (33). Progressive oral gangrene in acatalasemic patients was the first clinical trait detected in 1952 by Takahara (59), and obviously this phenomenon is the result of infection with H_2O_2-generating bacteria (mostly streptococci and pneumococci) or the action of phagocytic cells (neutrophils). In a similar way, all other traits are caused by abnormal levels of hydrogen peroxide not sufficiently removed by the mutated/altered catalase. A distinct polymorphism in the catalase gene sequence was described (33). Benign polymorphism in the catalase gene is represented by 22 detected base substitutions located in noncoding, flanking, and intron regions (35) as well as mutations of the third codon positions with no change in the amino acid sequence (53).

A relation between inherited catalase deficiency and diabetes mellitus in patients with type 1 diabetes was described in detail (19). Different deleterious mutations, formed mainly by single or double base insertions, missense mutations, and substitutions in the catalase gene, result in a dramatic decrease of blood catalase activity connected with increased hydrogen peroxide concentrations in serum and tissues. As a consequence, damage of the oxidation-sensitive insulin-producing pancreatic β cells has been reported. Other malign mutations in the catalase gene can affect the lipid, homocysteine, and erythrocyte metabolism (34) and give rise to hypertension (49) and vitiligo (15). Vitiligo is a complex genetic trait associated with genes responsible for melanin biosynthesis, response to oxidative stress, and regulation of autoimmunity. The epidermis of patients with vitiligo exhibits decreased catalase activity (33).

In last decade, a new aspect of catalase-related diseases and therapy has been investigated. Whereas most of the previous therapies dealt with catalase deficiency, now compelling evidence indicates that catalase overexpression can have adverse physiologic effects (see 83 for more details). Most of this knowledge comes from *in vitro* and *in vivo* experiments on mammalian cell lines, whereas in prokaryotes and lower eukaryotes, the direct evidence for this phenomenon is still missing. In human keratinocytes, hydrogen peroxide has been reported to support wound healing by inducing a specific vascular endothelial growth factor (82). Corresponding *in vivo* experiments on male mice revealed that adenoviral catalase gene delivery significantly impaired wound angiogenesis and closure. Moreover, catalase overexpression slowed tissue remodeling (80, 83). Obviously, this aspect of catalase overexpression also must be taken into consideration in the therapy for acatalasemic patients.

The mitochondrial–lysosomal axis theory of aging (93), a variant of the free radical theory of aging, proposes that accumulation of damage to mitochondria and especially to mitochondrial DNA leads to aging in mammals. This theory was supported by observations of increased accumulation of mutations in mitochondrial DNA, which is not protected by histones (as is the case for nuclear DNA). Such mutations occur mainly because of increased levels of activated oxygen species in aged mitochondria, resulting in loss of cellular energy, failures in cellular functions (10), and finally, phenoptosis. Recent results demonstrate an increase in health and lifespan after upregulation and overexpression of catalase imported in mouse mitochondria (21). This underlines the importance of future investigations on catalase that could lead to important new medical and biotechnologic applications.

Acknowledgments

This work was supported by the Austrian Science Foundation FWF (projects P19793 to M.Z. and P18751 to C.O.).

Abbreviations

AH_2	one-electron donor
CAT	gene coding for typical catalase
HPII	hydroperoxidase II (heme catalase)]
IPR	InterPro accession number identification at EBI database (U.K.)
KatA	typical (bacterial) catalase
KatG	catalase–peroxidase
LGT	lateral gene transfer

NDK-1	diphosphate kinase
OxyR	positive regulator for oxidative stress–inducible genes
PCC	Pasteur culture collection
PF	protein family
pfam	protein family
ROS	reactive oxygen species

References

1. Alfonso-Prieto M, Borovik A, Carpena X, Murshudov G, Melik-Adamyan W, Fita I, Rovira C, Loewen PC. The structures and electronic configuration of compound I intermediates of *Helicobacter pylori* and *Penicillium vitale* catalases determined by X-ray crystallography and WM/MM density functional theory calculations. J Am Chem Soc. 2007; 129:4193–4205. [PubMed: 17358056]
2. Antonyuk SV, Melik-Adamyan VR, Popov AN, Lamzin VS, Hempstead PD, Harrison PM, Artymiuk PJ, Barynin VV. Three-dimensional structure of the enzyme dimanganese catalase from *Thermus thermophilus* at 1A resolution. Crystallogr Rep. 2000; 45:105–116.
3. Baker RD, Cook CO, Goodwin DC. Properties of catalase-peroxidase lacking its C-terminal domain. Biochem Biophys Res Commun. 2004; 320:833–839. [PubMed: 15240123]
4. Barynin VV, Whittaker MM, Antonyuk SV, Lamzin VS, Harrison PM, Artymiuk PJ, Whittaker JW. Crystal structure of manganese catalase from *Lactobacillus plantarum*. structure. 2001; 9:725–738. [PubMed: 11587647]
5. Bayne ACV, Mockett RJ, Orr WC, Sohal RS. Enhanced catabolism of mitochondrial superoxide/hydrogen peroxide and aging in transgenic. Drosophila. Biochem J. 2005; 391:277–284.
6. Benecky MJ, Frew JE, Scowen N, Jones P, Hoffman BM. EPR and ENDOR detection of compound I from *Micrococcus lysodeikticus* catalase. Biochemistry. 1993; 32:11929–11933. [PubMed: 8218266]
7. Bertrand T, Eady NAJ, Jones JN, Jesmin JM, Nagy JM, Jamart-Gregoire B, Raven EL, Brown KA. Crystal structure of *Mycobacterium tuberculosis* catalase-peroxidase. J Biol Chem. 2004; 279:38991–38999. [PubMed: 15231843]
8. Bravo J, Fita I, Ferrer J, Ens W, Hillar A, Switala J, Loewen PC. Identification of a novel bond between a histidine and the essential tyrosine in catalase HPII of *Escherichia coli*. Protein Sci. 1997; 6:1016–1023. [PubMed: 9144772]
9. Brioukhanov AL, Netrusov AI. Catalase and superoxide dismutase: distribution, properties, and physiological role in cells of strict anaerobes. Biochemistry (Moscow). 2004; 69:949–962. [PubMed: 15521809]
10. Brunk UT, Terman A. The mitochondrial-lysosomyl axis theory of aging. Eur J Biochem. 2002; 269:1996–2002. [PubMed: 11985575]
11. Cabiscol E, Tamarit J, Ros J. Oxidative stress in bacteria and protein damage by reactive oxygen species. Int Microbiol. 2000; 3:3–8. [PubMed: 10963327]
12. Carpena X, Loprasert S, Mongkolsuk S, Switala J, Loewen PC, Fita I. Catalase-peroxidase KatG of *Burkholderia pseudomallei* at 1.7 A resolution. J Mol Biol. 2003; 327:475–489. [PubMed: 12628252]
13. Carpena X, Melik-Adamyan W, Loewen PC, Fita I. Structure of the C-terminal domain of the catalase-peroxidase KatG from *Escherichia coli*. Acta Crystallogr D. 2004; 60:1824–1832. [PubMed: 15388929]
14. Carpena X, Soriano M, Klotz MG, Duckworth HW, Donald LJ, Melik-Adamyan W, Fita I, Loewen PC. Structure of the clade 1 catalase, CatF of *Pseudomonas syringae*, at 1.8 Å resolution. Proteins: structure, function, and bioinformatics. 2003; 50:423–436.

15. Casp CB, She JX, McComack WT. Genetic association of the catalase gene (CAT) with vitiligo susceptibility. Pigment Cell Res. 2002; 15:62–66. [PubMed: 11837458]
16. Chelikani P, Carpena X, Fita I, Loewen PC. An electrical potential in the access channel of catalases enhances catalysis. J Biol Chem. 2003; 278:31290–31296. [PubMed: 12777389]
17. Chelikani P, Fita I, Loewen PC. Diversity of structures and properties among catalases. Cell Mol Life Sci. 2004; 61:192–208. [PubMed: 14745498]
18. Chouchane S, Girotto S, Shengwei Y, Magliozzo RS. Identification and characterization of tyrosyl radical formation in: *Mycobacterium tuberculosis* catalase-peroxidase (KatG). J Biol Chem. 2002; 277:42633–42638. [PubMed: 12205099]
19. Chystakov DA, Savastyanov KV, Chugunova LA. Association study of C167T polymorphism of the catalase gene and D6S392 locus nearby the Mn-dependent superoxide dismutase gene with diabetic microangiopathy. Ter Arkh. 2002; 74:28–30.
20. Crawford DR, Miralt ME, Moret R. Molecular defect in human acatalasia fibroblast. Biochem Biophys Res Commun. 1988; 153:59–66. [PubMed: 3377795]
21. Cutler RG. Oxidative stress and aging: catalase is a longevity determinant enzyme. Rejuvenat Res. 2005; 8:138–140.
22. de Groot H, Auferkamp O, Bramey T, de Groot K, Kirsch M, Korth HG, Petrat F, Sustmann R. Non-oxygen-forming pathways of hydrogen peroxide degradation by bovine liver catalase at low hydrogen peroxide fluxes. Free Radic Res. 2006; 40:67–74. [PubMed: 16298761]
23. de Visser SP. What external perturbations influence the electronic properties of catalase compound I? Inorg Chem. 2006; 45:9551–9557. [PubMed: 17083257]
24. Díaz A, Horjales E, Rudino-Pinera E, Arreola R, Hansberg W. Unusual Cys-Tyr covalent bond in a large catalase. J Mol Biol. 2004; 342:971–985. [PubMed: 15342250]
25. Donald LJ, Krokhin OV, Duckworth HW, Wiseman B, Deemagarn T, Singh R, Switala J, Carpena X, Fita I, Loewen PC. Characterization of the catalase-peroxidase KatG from *Burkholderia pseudomallei* by mass spectrometry. J Biol Chem. 2003; 278:35687–35692. [PubMed: 12832453]
26. Dos Santos WG, Pacheco I, Liu MY, Teixeira M, Xavier AV, LeGall J. Purification and characterization of an iron superoxide dismutase and a catalase from the sulfate-reducing bacterium *Desulfovibrio gigas*. J Bacteriol. 2000; 182:796–804. [PubMed: 10633116]
27. Engelmann S, Hecker M. Impaired oxidative stress resistance of *Bacillus subtilis* sigB mutants and the role of katA and katE. FEMS Microbiol Lett. 1996; 145:63–69. [PubMed: 8931328]
28. Fita I, Rossmann MG. The active center of catalase. J Mol Biol. 1985; 185:21–37. [PubMed: 4046038]
29. Gaetani GF, Ferraris AM, Rolfo M, Kirkman HN. Predominant role of catalase in the disposal of hydrogen peroxide within human erythrocytes. Blood. 1996; 87:1595–1599. [PubMed: 8608252]
30. Gaetani GF, Ferraris AM, Sanna P, Kirkman HN. A novel NADPH:(bound) $NADP^+$ reductase and NADH: (bound) $NADP^+$ transhydrogenase function in bovine liver catalase. Biochem J. 2005; 385:763–768. [PubMed: 15456401]
31. Ghiladi RA, Knudsen GM, Medzihradszky KF, de Montellano PR Ortiz. The Met-Tyr-Trp cross-link in *Mycobacterium tuberculosis* catalase-peroxidase (KatG): autocatalytic formation and effect on enzyme catalysis and spectroscopic properties. J Biol Chem. 2005; 280:22651–22663. [PubMed: 15840564]
32. Góth L, Rass P, Páy A. A new type of inherited catalase deficiencies: its characterization and comparison to the Japanese and Swiss type of acatalasemia. Blood Cells Mol Dis. 2001; 27:512–517. [PubMed: 11500062]
33. Góth L, Rass P, Páy A. Catalase enzyme mutations and their association with diseases. Mol Diagn. 2004; 8:141–149. [PubMed: 15771551]
34. Góth L, Vitai M. The effect of hydrogen peroxide promoted by homocysteine and inherited catalase deficiencyin human hypocatalasemic patients. Free Radic Biol Med. 2003; 31:490–498.
35. Góth L, Vitai M, Rass P, Sükei E, Páy A. Detection of a novel familial catalase mutation (Hungarian type D) and the possible risk of inherited catalase deficiency for diabetes mellitus. Electrophoresis. 2005; 26:1646–1649. [PubMed: 15800961]
36. Gouet P, Jouve HM, Dideberg O. Crystal structure of *Proteus mirabilis* PR catalase with and without bound NADPH. J Mol Biol. 1995; 249:933–954. [PubMed: 7791219]

37. Hakansson KO, Brugna M, Tasse L. The three-dimensional structure of catalase from *Enterococcus faecalis*. Acta Crystallogr D. 2004; 60:1374–1380. [PubMed: 15272159]
38. Hara I, Ichise N, Kojima K, Kondo H, Ohgiya S, Matsuyama H, Yumoto I. Relationship between the size of the bottleneck 15 Å from iron in the main channel and the reactivity of catalase corresponding to the molecular size of substrates. Biochemistry. 2007; 46:11–22. [PubMed: 17198371]
39. Heering HA, Indiani C, Regelsberger G, Jakopitsch C, Obinger C, Smulevich G. New insights into the heme cavity structure of catalase-peroxidase: a spectroscopic approach to the recombinant *Synechocystis* enzyme and selected distal cavity mutants. Biochemistry. 2002; 41:9237–9247. [PubMed: 12119039]
40. Hillar A, Nicholls P, Switala J, Loewen PC. NADPH binding and control of catalase compound II formation: comparison of bovine, yeast, and *Escherichia coli* enzymes. Biochem J. 1994; 300:521–539.
41. Hong Y, Wang G, Maier RJ. A *Helicobacter hepaticus* catalase mutant is hypersensitive to oxidative stress and suffers increased DNA damage. J Med Microbiol. 2007; 56:557–562. [PubMed: 17374900]
42. Ivancich A, Jakopitsch C, Auer M, Un S, Obinger C. Protein-based radicals in the catalase-peroxidase of *Synechocystis* PCC6803: a multifrequency EPR investigation of wild-type and variants on the environment of the heme active site. J Am Chem Soc. 2003; 125:14093–14102. [PubMed: 14611246]
43. Jakopitsch C, Auer M, Ivancich A, Ruker F, Furtmuller PG, Obinger C. Total conversion of bifunctional catalase-peroxidase (KatG) to monofunctional peroxidase by exchange of a conserved distal side tyrosine. J Biol Chem. 2003; 278:20185–20191. [PubMed: 12649295]
44. Jakopitsch C, Ivancich A, Schmuckenschlager F, Wanasinghe A, Pöltl G, Furtmüller PG, Rüker F, Obinger C. Influence of the unusual covalent adduct on the kinetics and formation of radical intermediates in *Synechocystis* catalase peroxidase. J Biol Chem. 2004; 279:46082–46095. [PubMed: 15326163]
45. Jakopitsch C, Kolarich D, Petutschnig G, Furtmüller PG, Obinger C. Distal side tryptophan, tyrosine and methionine in catalase-peroxidases are covalently linked in solution. FEBS Lett. 2003; 552:135–140. [PubMed: 14527675]
46. Jakopitsch C, Regelsberger G, Furtmüller PG, Rüker F, Peschek GA, Obinger C. Catalase-peroxidase from synechocystis is capable of chlorination and bromination reactions. Biochem Biophys Res Commun. 2001; 287:682–687. [PubMed: 11563849]
47. Jakopitsch C, Vlasits J, Wiseman B, Loewen PC, Obinger C. Redox intermediates in the catalase cycle of catalase-peroxidases from *Synechocystis* PCC 6803, *Burkholderia pseudomallei*, and *Mycobacterium tuberculosis*. Biochemistry. 2007; 46:1183–1193. [PubMed: 17260948]
48. Jamet A, Sigaud S, Van de Sype G, Puppo A, Hérouart D. Expression of the bacterial catalase genes during *Sinorhizobium melioti-Medicago sativa* symbiosis and their crucial role during the infection process. Mol Plant Microbe Interact. 2003; 16:217–225. [PubMed: 12650453]
49. Jiang Z, Akey JM, Shi J. A polymorphism in the promoter region of catalase is associated with blood pressure. Hum Genet. 2001; 109:95–98. [PubMed: 11479740]
50. Jones DP. Redefining oxidative stress. Antioxid Redox Signaling. 2006; 8:1865–1879.
51. Kalko SG, Gelpí JL, Fita I, Oroczo M. Theorethical study of the mechanisms of substrate recognition by catalase. J Am Chem Soc. 2001; 123:9665–9672. [PubMed: 11572688]
52. Kirkman HN, Gaetani GF. Mammalian catalase: a venerable enzyme with new mysteries. Trends Biochem Sci. 2007; 32:44–50. [PubMed: 17158050]
53. Kishimoto Y, Murakami Y, Hayashi K. Detection of a common mutation of the catalase gene in Japanese acatalasemic patients. Hum Genet. 1992; 88:487–490. [PubMed: 1551654]
54. Klotz MG, Loewen PC. The molecular evolution of catalatic hydroperoxidases: evidence for multiple lateral transfer of genes between prokaryota and from bacteria into eukaryota. Mol Biol Evol. 2003; 20:1098–1112. [PubMed: 12777528]
55. Kragler F, Langeder A, Raupachova J, Binder M, Hartig A. Two independent peroxisomal targeting signals in catalase A of *Saccharomyces cerevisiae*. J Cell Biol. 1993; 120:665–673. [PubMed: 8425895]

56. Levy E, Eval Z, Hochman A. Purification and characterization of a catalase-peroxidase from the fungus *Septoria tritici*. Arch Biochem Biophys. 1992; 296:321–327. [PubMed: 1605641]
57. Long SR. Rhizobium-legume nodulation: life together in the underground. Cell. 1989; 56:203–214. [PubMed: 2643474]
58. Magbanua ZV, De Moraes CM, Brooks TD, Williams WP, Luthe DS. Is catalase activity one of the factors associated with maize resistance to *Aspergillus flavus?* Mol Plant Microbe Interact. 2007; 20:697–706. [PubMed: 17555277]
59. Masuoka N, Sugiyama H, Ishibashi N, Wang DH, Masuoka T, Kodama H, Nakano T. Characterization of acatalasemic erythrocytes treated with low and high dose hydrogen peroxide: hemolysis and aggregation. J Biol Chem. 2006; 281:21728–21734. [PubMed: 16751193]
60. Mate MJ, Sevinc MS, Hu B, Bujons J, Bravo J, Switala J, Ens W, Loewen PC, Fita I. Mutants that alter the covalent structure of catalase hydroperoxidase II from *Escherichia coli*. J Biol Chem. 1999; 274:27717–27725. [PubMed: 10488114]
61. Mate MJ, Zamocky M, Nykyri LM, Herzog C, Alzari PM, Betzel C, Koller F, Fita I. Structure of catalase-A from *Saccharomyces cerevisiae*. J Mol Biol. 1999; 286:135–149. [PubMed: 9931255]
62. Mulvey MR, Switala J, Borys A, Loewen PC. Regulation of transcription of katE and katF in *Escherichia coli*. J Bacteriol. 1990; 172:6713–6720. [PubMed: 2254248]
63. Murshudov G, Melik-Adamyan VR, Grebenko AI, Barynin V, Vagin AA, Vainshtein BK, Dauter Z, Wilson KS. Three-dimensional structure of catalase from *Micrococus lysodeikticus* at 1.5 Å resolution. FEBS Lett. 1992; 312:127–131. [PubMed: 1426241]
64. Nicholls P, Fita I, Loewen PC. Enzymology and structure of catalases. Adv Inorg. Chem. 2001; 51:51–106.
65. Ogata M. Acatalasemia. Hum Genet. 1991; 86:331–340. [PubMed: 1999334]
66. Oldham ML, Brash AR, Newcomer ME. The structure of coral allene oxide synthase reveals a catalase adapted for metabolism of a fatty acid hydroperoxide. Proc Natl Acad Sci U S A. 2005; 102:297–302. [PubMed: 15625113]
67. Paris S, Wysong D, Debeaupuis J-P, Shibuya K, Philippe B, Diamond RD, Latgé J-P. Catalases of *Aspergillus fumigatus*. Infect Immun. 2003; 71:3551–3562. [PubMed: 12761140]
68. Passardi F, Theiler G, Zamocky M, Cosio C, Rouhier N, Teixera F, Margis-Pinheiro M, Ioannidis V, Penel C, Falquet L, Dunand C. PeroxiBase: the peroxidase database. Phytochemistry. 2007; 68:1605–1611. [PubMed: 17544465]
69. Passardi F, Zamocky M, Favet J, Jakopitsch C, Penel C, Obinger C, Dunand C. Phylogenetic distribution of catalase-peroxidases: are there patches of order in chaos? Gene. 2007; 397:101–113. [PubMed: 17561356]
70. Perelman A, Uzan A, Hacohen D, Schwarz R. Oxidative stress in *Synechococcus* sp. strain PCC 7942: various mechanisms for H_2O_2 detoxification with different physiological roles. J Bacteriol. 2003; 185:3654–3660. [PubMed: 12775703]
71. Petrova VY, Drescher D, Kujumdzieva AV, Schmitt MJ. Dual targeting of yeast catalase A to peroxisomes and mitochondria. Biochem J. 2004; 380:393–400. [PubMed: 14998369]
72. Peus D, Meves A, Vasa RA, Beyerle A, O'Brien T, Pettelkow MR. H_2O_2 is required for UVB-induced EGF receptor and downstream signaling pathway activation. Free Radic Biol Med. 1999; 27:1197–1202. [PubMed: 10641711]
73. Pongpom P, Cooper CR Jr, Vanittanakom N. Isolation and characterization of a catalase-peroxidase gene from the pathogenic fungus, *Penicillium marneffei*. Med Mycol. 2005; 43:403–411. [PubMed: 16178368]
74. Putnam CD, Arvai AS, Bourne Y, Tainer JA. Active and inhibited human catalase structures: ligand and NADPH binding and catalytic mechanism. J Mol Biol. 2000; 296:295–309. [PubMed: 10656833]
75. Radi R, Turrens JF, Chang LY, Bush KM, Crapo JD, Freeman BA. Detection of catalase in rat heart mitochondria. J Biol Chem. 1991; 266:22028–22034. [PubMed: 1657986]
76. Rahman I, Adcock IM. Oxidative stress and redox regulation of lung inflammation in COPD. Eur Respir J. 2006; 28:219–242. [PubMed: 16816350]

77. Regelsberger G, Jakopitsch C, Engleder M, Ruker F, Peschek GA, Obinger C. Spectral and kinetic studies of the oxidation of monosubstituted phenols and anilines by recombinant *Synechocystis* catalase-peroxidase compound I. Biochemistry. 1999; 38:10480–10488. [PubMed: 10441144]

78. Riise EK, Lorentzen MS, Helland R, Smalas AO, Leiros HKS, Willassen NP. The first structure of a cold-active catalase from *Vibrio salmonicida* at 1.96 Å reveals structural aspects of cold adaptation. Acta Crystallogr D. 2007; 63:135–148. [PubMed: 17242507]

79. Rocha ER, Selby T, Coleman JP, Smith CJ. Oxidative stress response in an anaerobe, *Bacteroides fragilis*: a role for catalase in protection against hydrogen peroxide. J Bacteriol. 1996; 178:6895–6903. [PubMed: 8955312]

80. Roy S, Khanna S, Nallu K, Hunt TK, Sen CK. Dermal wound healing is subject to redox control. Mol Ther. 2006; 13:211–220. [PubMed: 16126008]

81. Salvi M, Battaglia V, Brunati AM, La Rocca N, Tibaldi E, Pietrangeli P, Marcocci L, Mondovi B, Rossi CA, Toninello A. Catalase takes part in rat liver mitochondria oxidative stress defense. J Biol Chem. 2007; 282:24407–24415. [PubMed: 17576767]

82. Sen CK, Khanna S, Babior BM, Hunt TK, Elison EC, Roy S. Oxidant-induced vascular endothelial growth factor expression in human keratinocytes and cutaneous wound healing. J Biol Chem. 2002; 277:33284–33290. [PubMed: 12068011]

83. Sen CK, Roy S. Redox signals in wound healing. Biochim Biophys Acta. 2008 doi:10.1016/j.bbagen. 2008.01.006.

84. Shima S, Sordel-Klippert M, Brioukhanov A, Netrusov A, Linder D, Thauer RK. Characterization of a heme-dependent catalase from *Methanobrevibacter arboriphilus*. Appl Environ Microbiol. 2001; 67:3041–3045. [PubMed: 11425719]

85. Sigaud S, Becquet V, Frendo P, Puppo A, Hérouart D. Differential regulation of two divergent *Sinorhizobium meliloti* genes for HPII-like catalases during free-living growth and protective role of both catalases during symbiosis. J Bacteriol. 1999; 181:2634–2639. [PubMed: 10198032]

86. Singh R, Wiseman B, Deemagarn T, Donald LJ, Duckworth HW, Carpena X, Fita I, Loewen PC. Catalase-peroxidases (KatG) exhibit NADH oxidase activity. J Biol Chem. 2004; 279:43098–43106. [PubMed: 15280362]

87. Smulevich G, Jakopitsch C, Droghetti E, Obinger C. Probing the structure and bifunctionality of catalase-peroxidase (KatG). J Inorg Biochem. 2006; 100:568–585. [PubMed: 16516299]

88. Spiegel K, De Grado WF, Klein ML. Structural and dynamical properties of manganese catalase and the synthetic DF1 and their implication for reactivity from classical molecular dynamics calculations. Proteins Struct Funct Bioinform. 2006; 65:317–330.

89. Sun Y, Colburn NH, Oberley LW. Depression of catalase gene expression after immortalization and transformation of mouse liver cells. Carcinogenesis. 1993; 14:1505–1510. [PubMed: 8353835]

90. Switala J, Loewen PC. Diversity of properties among catalases. Arch Biochem Biophys. 2002; 401:145–154. [PubMed: 12054464]

91. Tamura K, Dudley J, Nei M, Kumar S. MEGA4: molecular evolutionary genetics analysis (MEGA) software version 4.0. Mol Biol Evol. 2007; 24:1596–1599. [PubMed: 17488738]

92. Terlecky SR, Koepke JI, Walton PA. Peroxisomes and aging. Biochim Biophs Acta. 2006; 1763:1749–1754.

93. Terman A, Brunk UT. Oxidative stress, accumulation of biological “garbage” and aging. Antioxid Redox Signal. 2006; 8:197–204. [PubMed: 16487053]

94. Teutloff C, Schäfer K-O, Sinnecker S, Barynin V, Bittl R, Wieghardt K, Lendzian F, Lubitz W. High-field EPR investigations of Mn(III)Mn(IV) and Mn(II)Mn(III) states of dimanganese catalase and related model systems. Magn Reson Chem. 2005; 43:S51–S64. [PubMed: 16235205]

95. Thomas JA, Morris DR, Hager LP. Chloroperoxidase VII: classical peroxidatic, catalatic, and halogenating forms of the enzyme. J Biol Chem. 1970; 245:3129–3134. [PubMed: 5432803]

96. Vainshtein BK, Melik-Adamyan VR, Barynin VV, Vagin AA, Grebenko AI, Borisov VV, Bartels KS, Fita I, Rossmann MG. Three-dimensional structure of catalase from *Penicillium vitale* at 2.0 Å resolution. J Mol Biol. 1986; 188:49–61. [PubMed: 3712443]

97. Veal EA, Day AM, Morgan BA. Hydrogen peroxide sensing and signaling. Mol Cell. 2007; 26:1–14. [PubMed: 17434122]

98. Vetrano AM, Heck DE, Mariano TM, Mishin V, Laskin DL, Laskin JD. Characterization of the oxidase activity in mammalian catalase. J Biol Chem. 2005; 280:35372–35381. [PubMed: 16079130]

99. Visser SP. What external perturbations influence the electronic properties of catalase compound I? Inorg Chem. 2006; 45:9551–9557. [PubMed: 17083257]

100. Wada K, Tada T, Nakamura Y, Kinoshita T, Tamoi M, Shigeoka S, Nishimura K. Crystallization and preliminary X-ray diffraction studies of catalase-peroxidase from *Synechococcus* PCC 7942. Acta Crystallogr D. 2002; 58:157–159. [PubMed: 11752798]

101. Wang N, Yoshida Y, Hasunuma K. Catalase-1 (CAT-1) and nucleoside diphosphate kinase-1 (NDK-1) play an important role in protecting conidial viability under light stress in *Neurospora crassa*. Mol Genet Genom. 2007; 278:235–242.

102. Welinder KG. Superfamily of plant, fungal, and bacterial peroxidases. Curr Opin Struct Biol. 1992; 2:388–393.

103. Whittaker MM, Barynin VV, Antonyuk SV, Whittaker JW. The oxidized (3,3) state of manganese catalase: comparison of enzymes from *Thermus thermophilus* and *Lactobacillus plantarum*. Biochemistry. 1999; 38:9126–9136. [PubMed: 10413487]

104. Whittaker MM, Barynin VV, Igarashi T, Whittaker JW. Outer sphere mutagenesis of *Lactobacillus plantarum* manganese catalase disrupts the cluster core. Eur J Biochem. 2003; 270:1102–1116. [PubMed: 12631270]

105. Wu S, Li Q, Du M, Shi-Yan L, Ren J. Cardiac-specific overexpression of catalase prolongs lifespan and attenuates ageing-induced cardiomyocyte contractile dysfunction and protein damage. Clin Exp Pharmacol Physiol. 2007; 34:81–87. [PubMed: 17201740]

106. Yamada Y, Fujiwara T, Sato T, Igarashi N, Tanaka N. The 2.0 Å crystal structure of catalase-peroxidase from *Haloarcula marismortui*. Nat Struct Biol. 2002; 9:691–695. [PubMed: 12172540]

107. Yano S, Arroyo N, Yano N. Catalase binds GRB2 in tumor cells when stimulated with serum or ligands for integrin receptors. Free Radic Biol Med. 2004; 36:1542–1554. [PubMed: 15182856]

108. Yano S, Yano N. Regulation of catalase enzyme activity by cell signaling molecules. Mol Cell Biochem. 2002; 240:119–130. [PubMed: 12487379]

109. Zamocky M, Jakopitsch C, Vlasits J, Obinger C. Fungal catalase-peroxidases: a novel group of bifunctional oxidoreductases. J Biol Inorg Chem. 2007; 12:S97.

110. Zamocky M, Koller F. Understanding the structure and function of catalases: clues from molecular evolution and in vitro mutagenesis. Prog Biophys Mol Biol. 1999; 72:19–66. [PubMed: 10446501]

111. Zamocky M, Regelsberger G, Jakopitsch C, Obinger C. The molecular peculiarities of catalase-peroxidases. FEBS Lett. 2001; 492:177–182. [PubMed: 11257490]

112. Zhao X, Yu H, Yu S, Wang F, Sacchettini JC, Magliozzo RS. Hydrogen peroxide-mediated isoniazid activation catalyzed by *Mycobacterium tuberculosis* catalase-peroxidase (KatG) and its S315T mutant. Biochemistry. 2006; 45:4131–4140. [PubMed: 16566587]

Europe PMC Funders Author Manuscripts

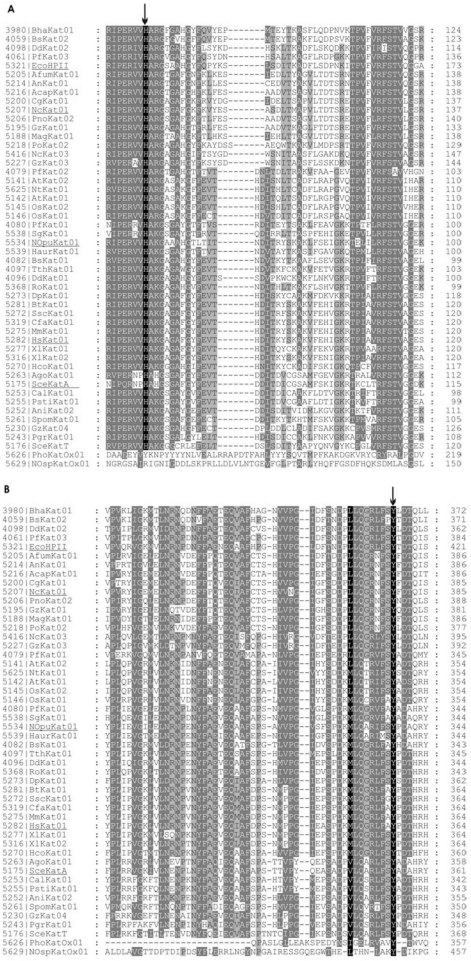

FIG. 1. Multiple sequence alignment of selected typical catalases

ClustalX, version 1.81, was used with Gonnet 250 protein weight matrix. Gap-opening penalty 9.00 and gap-extension penalty 0.20 was used in slow-accurate alignment algorithm. Residue-specific penalties and hydrophilic penalties were activated, and the gap-separation distance was optimised to 8. (**A**) Distal side of the prosthetic heme group. (**B**) Proximal side of heme with essential tyrosine. *Black*, Similarity scheme with highest similarity; *dark grey*, high similarity; *light grey*, low similarity; *arrow*, catalytically important residues. Abbreviations for Linnaean names and ID numbers correspond to PeroxiBase nomenclature (68; see http://peroxibase.isb-sib.ch/ for all details).

Europe PMC Funders Author Manuscripts

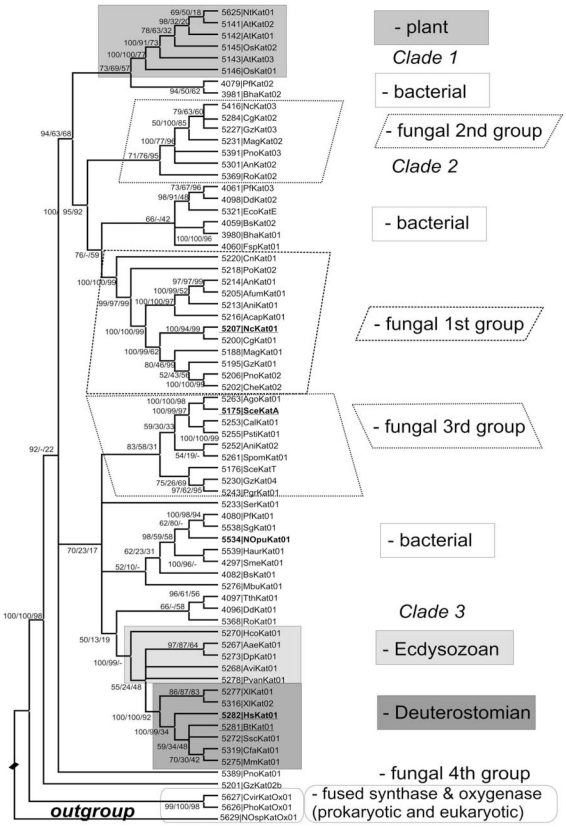

FIG. 2. Reconstructed phylogenetic tree of 70 typical catalases from all main living kingdoms

Presented is the tree obtained with the neighbor-joining method and 1,000 bootstrap cycles. Very similar trees were reconstructed also with maximum parsimony (1,000 bootstraps) and maximum likelihood (100 bootstraps) methods. Rooting of the tree was performed by using the fused synthase and oxygenase sequence as an outgroup. Numbers on the branches represent bootstrap values for NJ/MP/ML methods, respectively. The phylogenetic relations were reconstructed by using MEGA4 (91) and Phylip packages (http://evolution.gs.washington.edu/phylip.html). For NJ and ML methods, the Jones-Taylor-Thornton protein matrix was used with an optimized γ parameter = 1.90. For the MP method, the CNI level was set to 1 with initial tree search by random addition with 10 replicates. The outgroup (for rooting purposes) is labeled with a rhombus. Sequences with known 3D structures are underlined. The groupings in major subfamilies are marked by different boxes with self-explanation on the right side.

Europe PMC Funders Author Manuscripts

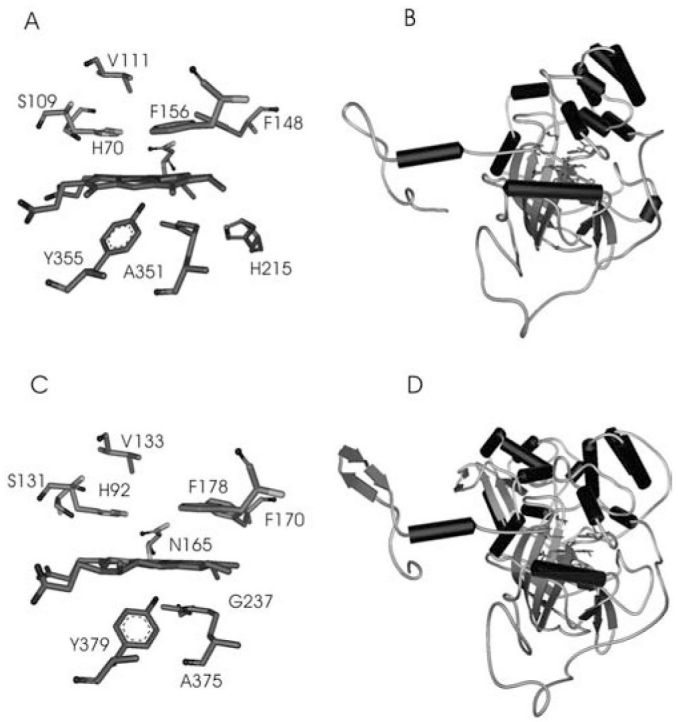

FIG. 3. Structural comparison of catalase A from *Saccharomyces cerevisiae* and catalase-1 from *Neurospora crassa*

(**A**) Heme-cavity architecture of catalase A from *Saccharomyces cerevisiae*. The conserved distal residues His70, Ser104, Val111, Asn143, Phe148, and Phe156 are shown; the proximal heme ligand is Tyr355, hydrogen-bonded to Arg375. The figure was constructed by using the coordinates deposited in the Protein Data Bank (accession code 1a4e). (**B**) Monomeric structure of catalase A from *Saccharomyces cerevisiae*, showing the assignment of secondary structure elements and the prosthetic group. (**C**) View of the active site of catalase-1 from *Neurospora crassa*, showing the conserved distal residues His92, Ser131, Val133, Asp165, Phe170, and Phe178, as well as the proximal residues Tyr379, Arg375, and Gly237. The figure was constructed by using the coordinates deposited in the Protein Data Bank (accession code 1sy7). (**D**) Monomeric structure of catalase-1 from *Neurospora crassa*, showing the assignment of secondary structure elements and the prosthetic group.

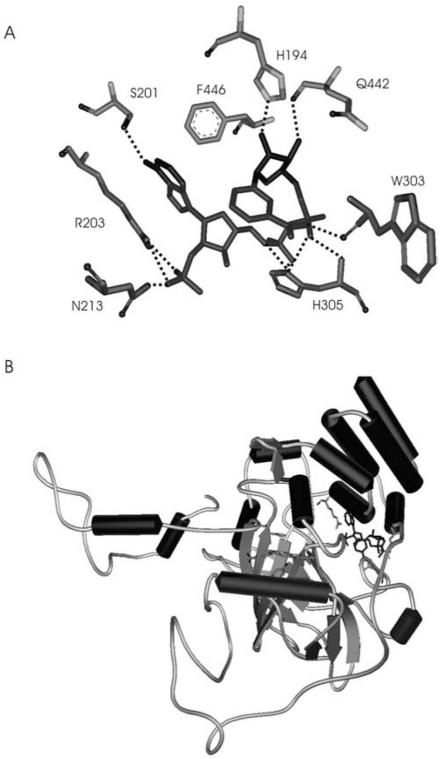

FIG. 4. Structure of NADPH-binding pocket in *Homo sapiens* catalase

(**A**) View showing the NADPH-binding pocket with residues that are involved in hydrogen bonding with NADPH. (**B**) Monomeric structure of catalase from *Homo sapiens*, showing the assignment of secondary structure elements and the NADPH-binding pocket. The figure was constructed by using the coordinates deposited in the Protein Data Bank (accession code 1dgb).

Europe PMC Funders Author Manuscripts

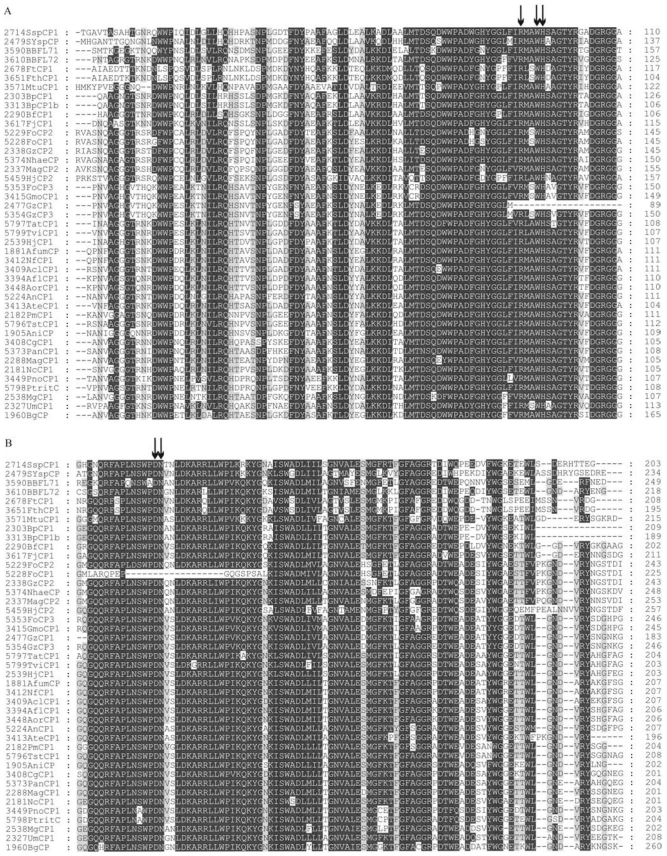

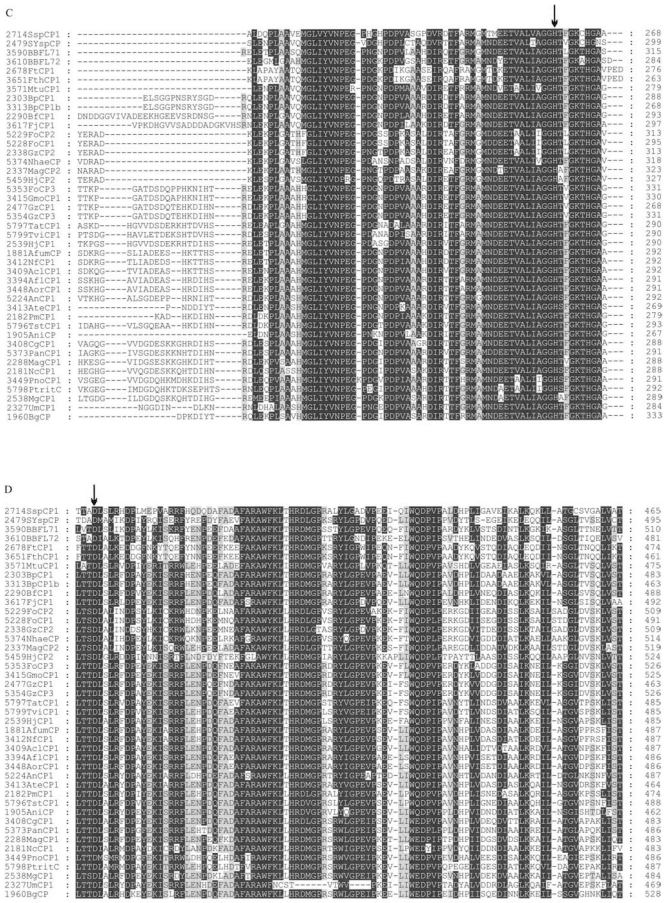

FIG. 5. Selected parts of the multiple sequence alignment of 43 catalase–peroxidases (KatGs)
Thirty-two complete fungal sequences are presented together with closely related bacterial counterparts. Similarity scheme is identical with that in Fig. 1. The substitution matrix and the alignment algorithm were the same as used in recent experimental work on this topic (69). (**A**) Distal side of the heme group with the catalytic triad. (**B**) Distal side of heme with important hydrogen bond location. (**C**) Proximal side of the prosthetic heme group with the essential histidine. (**D**) Proximal side of heme with important hydrogen bond location. *Arrow*, Catalytically important residues. Abbreviations for Linnaean names and ID numbers correspond to PeroxiBase nomenclature (68; see http://peroxibase.isb-sib.ch/ for all details).

Europe PMC Funders Author Manuscripts

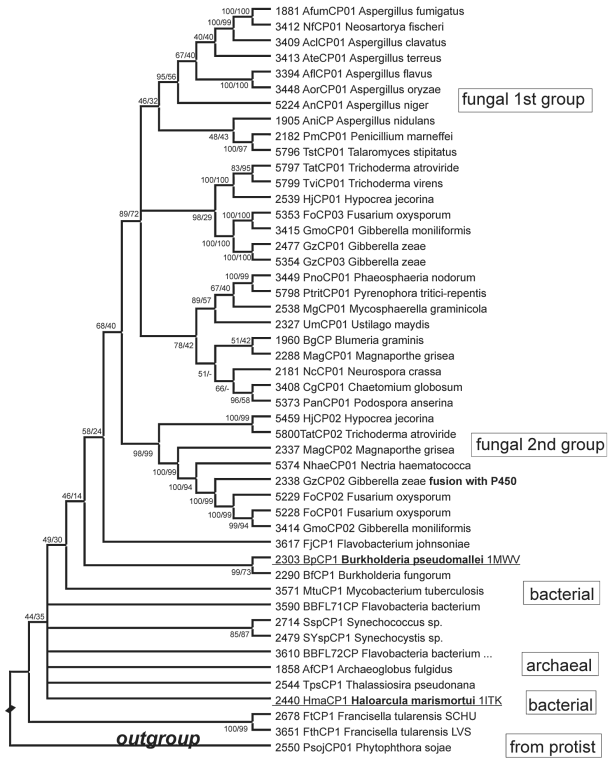

FIG. 6. Reconstructed phylogenetic tree of bacterial and fungal KatGs obtained with the neighbor-joining method and 1,000 bootstrap replications

An almost identical tree was obtained with maximum parsimony method by using 1,000 bootstrap replications. The phylogenetic relations were reconstructed by using the MEGA4 software package (91). The optimized parameters for the NJ and MP methods were the same as those used in recent experimental work on this topic (69). Numbers on the branches represent bootstrap values for NJ/MP methods, respectively. Sequences with known 3D structures are underlined. The outgroup is labeled with a rhombus.

Europe PMC Funders Author Manuscripts

Europe PMC Funders Author Manuscripts

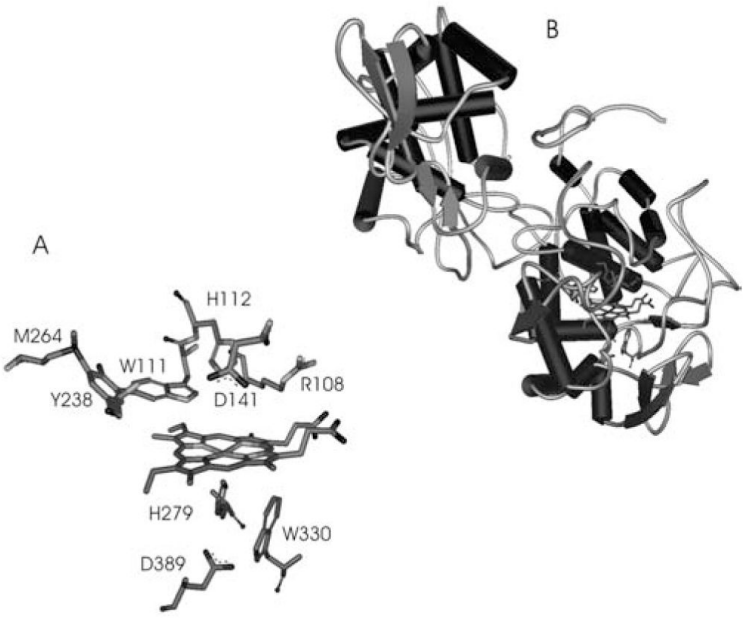

FIG. 7. Structure of catalase–peroxidase from *Burkholderia pseudomallei*

(**A**) Distal active residues are covalent linked Met264, Tyr238, and Try111, the catalytically active His112, Arg108, and Asp141 that contribute to the stabilization of the H-bonding network of the access channel. (**B**) Monomeric structure of catalase–peroxidase from *Burkholderia pseudomallei* showing the assignment of secondary structure elements and the prosthetic group. The figure was constructed by using the coordinates deposited in the Protein Data Bank (accession code 1mwv).

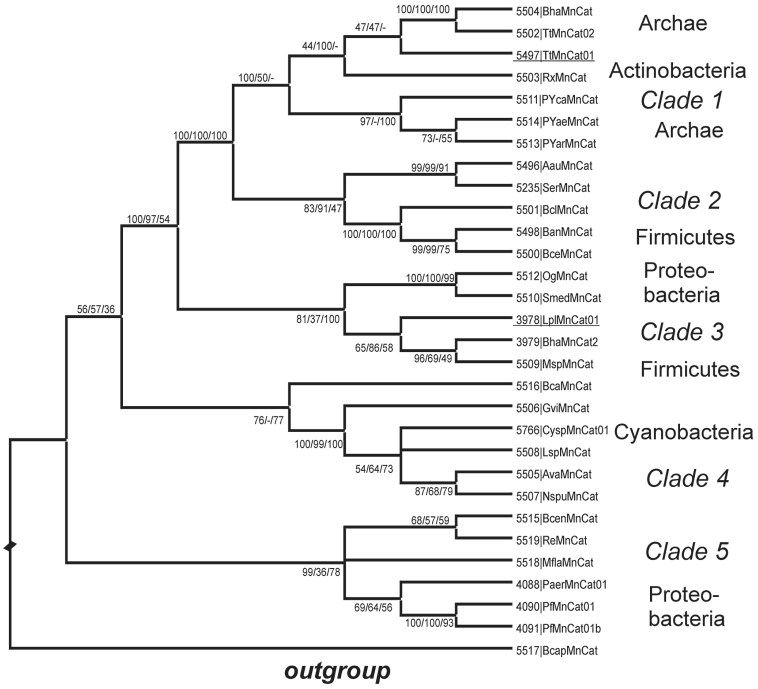

FIG. 8. Inferred phylogenetic tree of 30 manganese catalases rooted with an outgroup

The phylogenetic relations were reconstructed by using MEGA4 (91) and Phylip packages (http://evolution.gs.washington.edu/phylip.html). Presented is the tree obtained with the neighbor-joining method and 1,000 bootstrap replications. Almost identical trees were obtained with maximum-parsimony and maximum-likelihood methods. Applied parameters were the same as those used for Fig. 2 (see earlier), with the only exception that uniform rates of substitutions were applied for NJ and ML methods. Numbers on the branches represent bootstrap values for NJ/MP/ML methods, respectively. Sequences with known 3D structures are underlined. The outgroup is labeled with a rhombus.

Europe PMC Funders Author Manuscripts

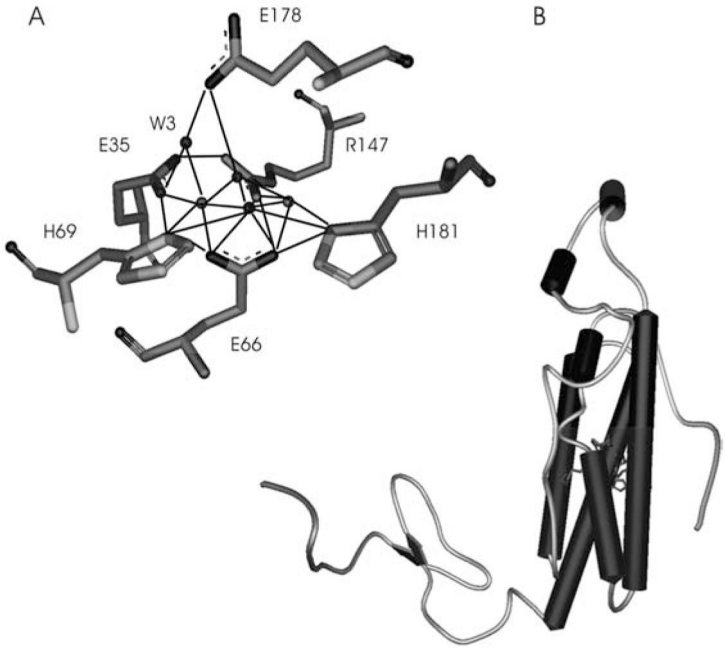

FIG. 9. Structure of manganese catalase of *Lactobacillus plantarum*

(**A**) View of the dinuclear manganese complex at the active site in *Lactobacillus plantarum*. All coordinating ligands are depicted. *Dark grey spheres*, Manganese ions; *light grey spheres*, Coordinated solvent. (**B**) Monomeric structure of Mn catalase from *Lactobacillus plantarum* showing the assignment of secondary structure elements and the prosthetic group. The figure was constructed by using the coordinates deposited in the Protein Data Bank (accession code 1jku).

Europe PMC Funders Author Manuscripts

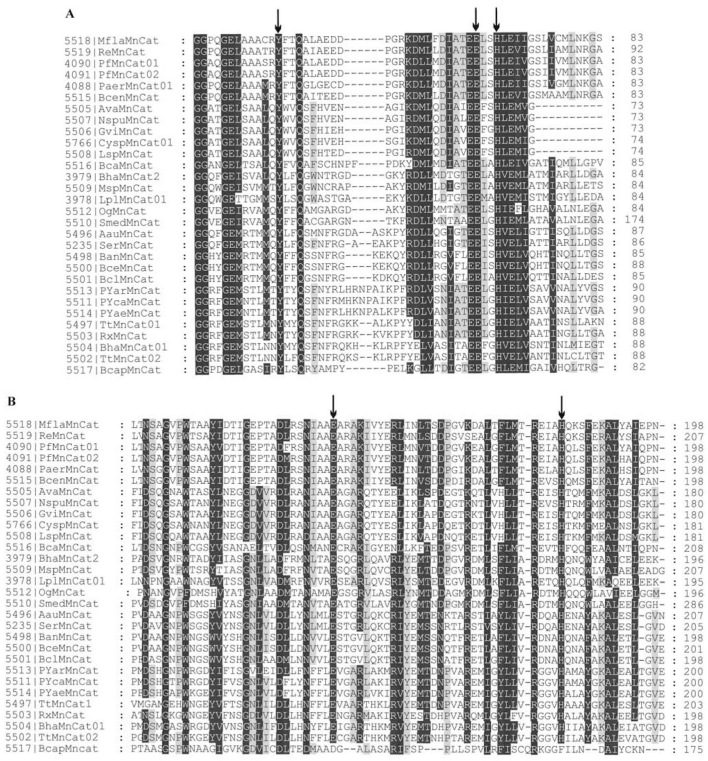

FIG. 10. Selected parts of multiple sequence alignment of 30 bacterial manganese catalases

ClustalX, version 1.81, was used with Gonet 250 protein weight matrix. Gap-opening penalty 8.00 and gap-extension penalty 0.20 were used in a slow-accurate algorithm. Residue-specific penalties and hydrophilic penalties were activated, and the gap-separation distance was optimized to 6. The similarity scheme is identical with that in Fig. 1. Abbreviations for Linnaean names and ID numbers correspond to PeroxiBase nomenclature (68; see http://peroxibase.isb-sib.ch/ for all details).

Europe PMC Funders Author Manuscripts

Europe PMC Funders Author Manuscripts

Antioxid Redox Signal. Author manuscript; available in PMC 2010 October 22.

TABLE 1

Overview of Known 3D-Structures of 14 Typical (Monofunctional) Catalases, 5 Catalase-Peroxidase (KatG) and 2 Mn-Catalases (as in December 2007)

PDB code	Source	Type	Reference
	Typical catalases		
1GGE	*Escherichia coli*	Large subunit, clade 2	8
1SI8	*Enterococcus faecalis*	Small subunit, clade 3	37
2A9E	*Helicobacter pylori*	Small subunit, clade 3	1
1M85	*Proteus mirabilis*	Small subunit, clade 3	36
1GWE	*Micrococcus lysodeikticus*	Small subunit, clade 3	63
1M7S	*Pseudomonas syringae*	Small subunit, clade 1	14
2ISA	*Vibrio salmonicida*	Small subunit, clade 1	78
2J2M	*Exiguobacterium oxidotolerans*	Small subunit, clade	38
1A4E	*Saccharomyces cerevisiae*	Small subunit, clade 3	61, Fig. 3 A,B
2IUF	*Penicillium vitale*	Large subunit, clade 2	96
1SY7	*Neurospora crassa*	Large subunit, clade 2	24, Fig. 3 C,D
1U5U	*Plexaura homomalla*	Small subunit, fused	66
8CAT	*Bos taurus* (liver)	Small subunit, clade 3	28
1DGB	*Homo sapiens* (erythrocyte)	Small subunit, clade 3	74, Fig. 4
	Catalase-peroxidases		
1ITK	*Haloarcula marismortui*	Archae KatG	106
1UB2	*Synechococcus* PCC 7942	Eubacterial KatG	100
1MWV	*Burkholderia pseudomallei*	Eubacterial KatG	12, Fig. 7
1U2K	*Escherichia coli*	Eubacterial KatG	13
1SJ2	*Mycobacterium tuberculosis*	Eubacterial KatG	7
	Mn-catalases		
1JKU	*Lactobacillus plantarum*	Clade 3	4, Fig. 9
2CWL	*Thermus thermophilus*	Clade 1	Ebihara *et al.*, unpublished; 2